Data in Brief Research Article

Mapping influenza-induced posttranslational modifications on histones from CD8+ T cells

Svetlana Rezinciuc[1], Sisi Wu[1], Shawna Hengel[1], Ljiljana Pasa-Tolic[1], and Heather S. Smallwood[1,3*]

[1]Department of Pediatrics, University of Tennessee Health Science Center, Memphis, Tennessee, USA
[2] Environmental Molecular Sciences Laboratory, Pacific Northwest National Laboratory, Richland, Washington, USA
[3] Children's Foundation Research Institute, Memphis, Tennessee, USA

* Correspondence: hsmallwo@uthsc.edu; +1 (901) 448-3068

Abstract: T cell function is determined by transcriptional networks that are regulated by epigenetic programming via posttranslational modifications (PTMs) of histone proteins and DNA. Bottom-up mass spectrometry (MS) can identify histone PTMs, whereas intact protein analysis with high-field Fourier transform ion cyclotron resonance MS (FTICR-MS) can detect species missed by bottom-up approaches. We used high-resolution reversed-phase liquid chromatography (RPLC) FTICR-MS, alternating electron transfer dissociation (ETD) and collision-induced dissociation (CID) on precursor ions to maximize fragmentation of uniquely modified species. First online RPLC separation sorted histone families then weak cation exchange hydrophilic interaction liquid chromatography (WCX-HILIC) separated species heavily clad in PTMs. Tentative PTM identifications were assigned by matching peptide masses to predicted theoretical masses that were verified with tandem MS. We used this innovative approach for Histone-intact protein PTM mapping (HiPTMap) and to quantify PTMs on core histones purified from CD8+ T cells directly isolated *ex vivo* post-influenza infection. Activation significantly reduced PTMs *in vivo* following influenza infection, histone maps changed as T cells migrated to infections, and T cells responding to secondary heterologous infections had significantly more PTMs enhancing transcriptional activation. Thus, HiPTMap identifies and quantifies PTMs on CD8+ T cell histones and determines their combinations in T cell states.

Keywords: epigenetic; histone; posttranslational modifications; T cells; influenza; FTICR; top-down; mass spectrometry

1. Introduction

Clearance of viral infection depends upon a well-orchestrated immune response and requires precise control of the immediate effector T cell response as well as the formation and maintenance of the memory cell population. Activation of naïve T cells initiates an autonomous program of differentiation and the acquisition of effector functions, including proinflammatory cytokine and cytolytic effector molecule production [1-5]. Cytotoxic $CD8^+$ T cells modulate their transcriptional programs as they adapt to activation and immune resolution stimuli, which influences their differentiation status and function. Thus, in response to dynamic environmental conditions, naïve cells alter their signaling cascades and pathways, leading to the induction of enzymes that control the epigenetic imprinting of CD8+ T cells [6]. These epigenetic imprints comprise posttranscriptional modifications (PTMs) to histones and DNA; these heritable changes circumvent altering primary DNA sequences [3, 7-12]. Indeed, T cells change histone PTMs at gene loci associated with effector function [3, 13-17]. After the resolution of viral infection, effector T cell populations contract, and a small population of pathogen-specific, long-lived memory cells. Memory T cells are imprinted during the primary response, and their robust recall response dictates the efficiency of the immune response to secondary infections. These virus-specific memory T cells are preprogrammed to rapidly respond to subsequent infections without further differentiation [5, 18-23]. It has long been appreciated that naïve, effector, and memory CD8+ T

 doi:10.20944/preprints202010.0215.v1

cells have distinct phenotypes and functions. However, we are just beginning to understand the underlying molecular mechanisms that control the maintenance of these subsets and their unique responses to infection.

Combinations of histone PTMs at discreet genomic locations can indicate transcription levels and regulate cell type-specific gene expression patterns [24, 25]. The protruding termini of histone tails represents the main PTM sites for acetylation, methylation, phosphorylation and ubiquitination that directly alter DNA accessibility or act indirectly via binding or chaperoning other proteins [26, 27]. Acetylation of lysine residues on histones reduces their positive charge, weakening the electrostatic interaction with DNA. This "permissive" state allows transcription factors to access genes in this region. Conversely, when histone deacetylases remove these PTMs, the structure condenses, thereby restricting access to the region [28]. Thus, these enzymes play central roles in controlling T cell development [29-31], regulatory function maintenance [32], CD8+ T cell proliferation [33], and effector functions, including the anti-viral response of antigen-specific CD8+ T cells [34, 35]. In contrast to the on/off effects of acetylation, the effects of histone methylation are context dependent. For example, trimethylation of histone 3 or 4 (H3 or H4) at lysine 4 or 9, respectively, is permissive, while the location and degree of methylation of H3 (H3K27me3, H3K9me3, H3K9me2) within gene loci typically correlates with transcriptional repression [25, 36-45]. This context dependency comes into play when both marks are present, which is called bivalent. Bivalent marks on H3 are thought to contribute to rapid T cell differentiation [46-48]. Mapping gene expression patterns at loci associated with H3K4me3 and H3K27me3 from naïve, effector, and memory CD8+ T cells revealed the expression of T cell lineage-defining genes correlated with phenotypic and functional differences between virus-specific CD8+ T cell subsets [3]. Following influenza infection, the transition from naïve to effector T cell was characterized by the loss of repressive H3K27me3 at specific bivalent loci and provided a mechanistic basis for the coordinate regulation of transcription during differentiation. Furthermore, a study of trimethylation at these sites within human polyclonal T cells showed specific methylation patterns correlated with subset-specific gene expression [17]. Whether changes in histone PTMs direct T cell differentiation and fate and the extent of epigenetic imprints on histones remains unclear. Identifying histone variants and their PTMs may elucidate their functional mechanisms in chromatin regulation in CD8+ T cells and may provide new insights into maintenance of T cell phenotypes.

H3 trimethylations are the most widely studied of the histone octamer. However, the octamer contains two H2A and H2B dimers as well as a tetramer of H3 and H4 proteins. Given the emerging role of epigenetics in CD8+ T cell regulation, deciphering the histone code is of immediate importance. Analyzing intact histones by top-down mass spectrometry (MS) is a major advantage because combinatorial patterns of modifications on a single histone molecule can be identified [49]. Here, we used two-dimensional liquid chromatography-MS/MS (2D LC-MS/MS) for histone-intact protein PTM mapping (HiPTMap) of H2A, H2B, H3, and H4 purified from CD8+ T cells following influenza infection. This approach allowed us to assess the dynamics of the PTM landscape in naïve and activated T cells in the primary infection; map PTMs as effector T cells migrated to the site of infection; and compare primary, memory, and secondary subsets. We identified 225 PTMs in these isoforms from the spleen, bronchial lavage fluid (BAL) and lungs and found distinct PTMs based on T cell activation. HiPTMap is particularly valuable for advancing our understanding of T cell biology by providing relative quantification of PTMs in different cell states with minimal histone protein. Furthermore, these results demonstrate this approach and technological advancements in MS are poised to increase the identification of novel modification locations and combinations that will generate a more complete map of the histone code in T cell differentiation. This information may also shed light on other regulatory mechanisms and loci relevant to T cell function.

2. Materials and Methods

Infections and T cell extraction

Female C57BL/6 mice (The Jackson Laboratory, Bar Harbor, ME, USA) were infected for 9 days for primary and ≥30 days for memory or secondary challenge. Mice were intranasally infected with influenza A virus (A/X-31(H3N2)) at $EID_{50} = 10^6$. For challenge, at least 30 days prior to X31 infection,

 doi:10.20944/preprints202010.0215.v1

mice received an intraperitoneal injection of A/Puerto Rico/8/1934 at $EID_{50} = 10^8$. Mice were sacrificed at specific times after X31 infection (9 days for primary, 7 days for secondary, and 30 days for memory). In each experiment, we used 2-5, 10-15, or 1-2 mice per group for the primary, memory, and secondary groups, respectively. Spleens were collected and CD8+ cells separated [5, 22, 50] using B220, MHCII, CD11b, and DX5 (NK) antibody cocktail (Miltenyi Biotec, Auburn, CA, USA). Fluorescence-activated cell sorting (FACS) was used to isolate CD8+ T cells. Activated splenic T cells were selected based on $CD8^{hi}$ $CD44^{hi}$ $CD43^{hi}$ $CD25^{hi}$, and naïve cells were selected based on $CD8^{hi}$ $CD44^{low}$ $CD43^{low}$ $CD25^{low}$. T cells from BAL were selected based on $CD8^{+}$ $CD44^{hi}$ $CD43^{hi+}$ $CD25^{+}$, Lung $CD8^{+}$ $CD44^{hi}$ $CD43^{hi}$ $CD25^{mid-hi}$. T cell pellets were resuspended in ammonium bicarbonate with protease inhibitor cocktail (Roche, Indianapolis, IN, USA). Histones were purified using a Histone Purification kit (Active Motif, Carlsbad, CA, USA) for purifying core histones while preserving modification states. Columns were poured for each group and kept constant. We followed the manufacturer's protocol for gravity flow separation of H2A, H2B, H3 and H4 core histones. Protein was purified from each group, and 9 μg protein per run was used for MS analysis. For relative comparisons (e.g., naïve -vs- active or active spleen-vs-BAL-vs-lung), mice and samples were treated as above except histones were pooled for relative quantification (10 mice each).

Mass spectra acquisition

We previously developed an optimized MS workflow for HiPTMap and provided a detailed MS configuration and separation strategy [51]. Briefly, purified histones (7.5-10 μg) were separated in the first dimension using a Jupiter C5 column (5-μm particles, 300 Å pore size, 600 mm × 200 μm i.d.) (Phenomenex, Torrance, CA, USA). Two Model 100 DM 10,000 psi syringe pumps (ISCO, Lincoln, NE, USA) were used to maintain constant pressure (4,000 psi) during separation. A gradient was generated by adding mobile phase B to a stirred mixer of mobile phase A (2.5 mL volume at 100% "A" at time zero). Mobile phase A was 20% acetonitrile (CAN) aqueous solution with 5% isopropyl alcohol (IPA) and 0.6% formic acid (FA). Mobile phase B was 45% ACN, 45% IPA, and 0.6% FA. The appropriate split flow rate was controlled by the combination of a packed column together with 15 μm i.d. capillary, with an approximate flow of 10 μL/min. We used a SPECTRA100 UV detector (Thermo Separation Products, Waltham, MA, USA) to monitor protein elution online at 214 nm, and fractions were collected using a Cheminert column selector system (VICI, Houston, TX, USA). This setup allowed for sequential selection of histone core members by group and second dimension separation by fraction.

Each histone family fraction was further separated in the second dimension by weak cation exchange hydrophilic interaction liquid chromatography (WCX-HILIC) using a 50 cm × 100 μm i.d. column prepared with PolyCAT A (5-μm particles, 1000 Å pore size) (PloyLC, Columbia, MD, USA). We used a 70% ACN aqueous solution with 1.0% FA for mobile phase A (2°A) and 70% ACN and 8% FA for mobile phase B (2°B) for the gradient in the second-dimension separation. To increase the throughput of the second dimension, we employed a ten-port Nanovolume injection valve (VICI) to house two capillary columns, enabling separation and concurrent loading/equilibration between the two columns. Each isolated core histone fraction was loaded onto a 150 μm i.d. × 5 cm solid-phase extraction column with HILIC stationary phase described above. After loading each fraction in mobile phase 2°A, mobile phase 2°B was added to the mixing vessel to separate the isoforms of each core histone. We then acquired spectra using electrospray ionization (ESI) high-resolution MS and MS/MS acquisitions in an LTQ Orbitrap Velos (ThermoFisher Scientific, Waltham, MA). ESI voltage was applied by connecting the end of the LC column to a capillary emitter with a polyetheretherketone (PEEK) union while voltage was applied [51]. Acquisitions with the Orbitrap had nominal resolving power of 60,000 (m/z = 400). FTMS MS and MSn gain control were set at 1E6 and 3E5, respectively, with three micro scans each. Precursor ion fragments were isolated with a 1.5 m/z window. The collision-induced dissociation (CID; normalized collision energy 35%, 30 ms) and electron transfer dissociation (ETD; reaction time 25 ms) for the same precursor ion were alternated, and an exclusion duration of 900 s and an exclusion list size of 150 were applied. MS/MS was only performed on species with charge states greater than four. Raw MS data for both dimensions were deposited in the PeptideAtlas repository (link available on publication).

 doi:10.20944/preprints202010.0215.v1

Data analysis

Protein isoforms as well as PTMs were identified by searching raw data against a mouse-specific annotated database, Mouse – Top down database (1260319 basic sequences, 5097711 protein forms), using ProSightPC 2.0 software (Thermo Scientific) using the Xtract algorithm and Top Down (MS2) default settings. The analysis was performed in single-protein search mode with dynamic modifications used for the identification of PTMs, including acetylation, mono-, di-, and trimethylation and phosphorylation with a mass tolerance of 10 ppm for precursor and 10 ppm for fragments using Δm mode (this function allows identification of proteoforms with PTMs not included in the annotated proteoform database). The minimum signal-to-noise (S/N), minimum reliability (RL), maximum charge and maximum mass were set to 1.0, 0.9, 40, and 25 kDa, respectively. Individual spectra were searched in absolute mass mode if a minimum of six fragments and minimum intact mass of 5,000 Da were observed, and the fragment mass tolerance was set at 10 ppm. Due to limitations in the ProSightPC search tool (i.e., restricted to previously annotated PTMs), manual analysis was performed in the few cases ProSightPC could not identify species in a region of import between biological comparisons. Histone identifications were filtered by requiring the 'Number of Best Hits' to be one (globally unique ID). The false discovery rate (FDR) was evaluated using a reversed database search with the same filtering criteria, where FDR = 100*Nreverse/Nforward. A P score cutoff of 0.00025 was chosen with FDR < 1%. MS Access was used as a platform to align and normalize individual histones from 2D display for further inference of LC-MS datasets of histone isoforms generated from T cell subsets.

3. Results

3.1. Naïve versus activated T cell histone modification

We used high-resolution reversed-phase liquid chromatography with tandem mass spectrometry (RPLC-MS/MS) on a Orbitrap Velos with alternating CID and ETD. We previously developed this technique using histones purified from HeLa cells and demonstrated the high sensitivity of this method for comprehensive characterization of histone PTMs [51]. Here we applied this MS method for HiPTMap of modifications that formed *in vivo* following intranasal infection with influenza virus. Both MS and MS/MS were detected with high resolution and mass tolerance (intact 1 Da and fragment ions of 10 ppm). All core histones were realized in the first dimension of seperation and seperated into individual family members H4, H2B, H2A, and H3 that appear in increasing order of hydrophobicity [Fig 1a-c]. Isoforms within each histone core family elute together except for H3, which elutes in two distinct peaks, and in order by increasing molecular weight (H4, H2B, H2A, and H3 are 11,352.5, 13,757.1, 14,019.9, and 15,350.8 Da, respectively). As one would expect with reversed-phase separation, each core histone group's elution time is also influenced by its hydrophobicity. Hence the seperation of H3 into two groups, whereby the species eluting in the second peak is characterized by up to three additional methylations that increase the hydrophobicity of these isoforms. This clear separation of histone core family members allows for facile separation, fragmentation, and downstream HiPTMap of proteins isolated from naïve and activated T cells.

Preprints (www.preprints.org) | NOT PEER-REVIEWED | Posted: 12 October 2020 doi:10.20944/preprints202010.0215.v1

[Figure 1 about here]

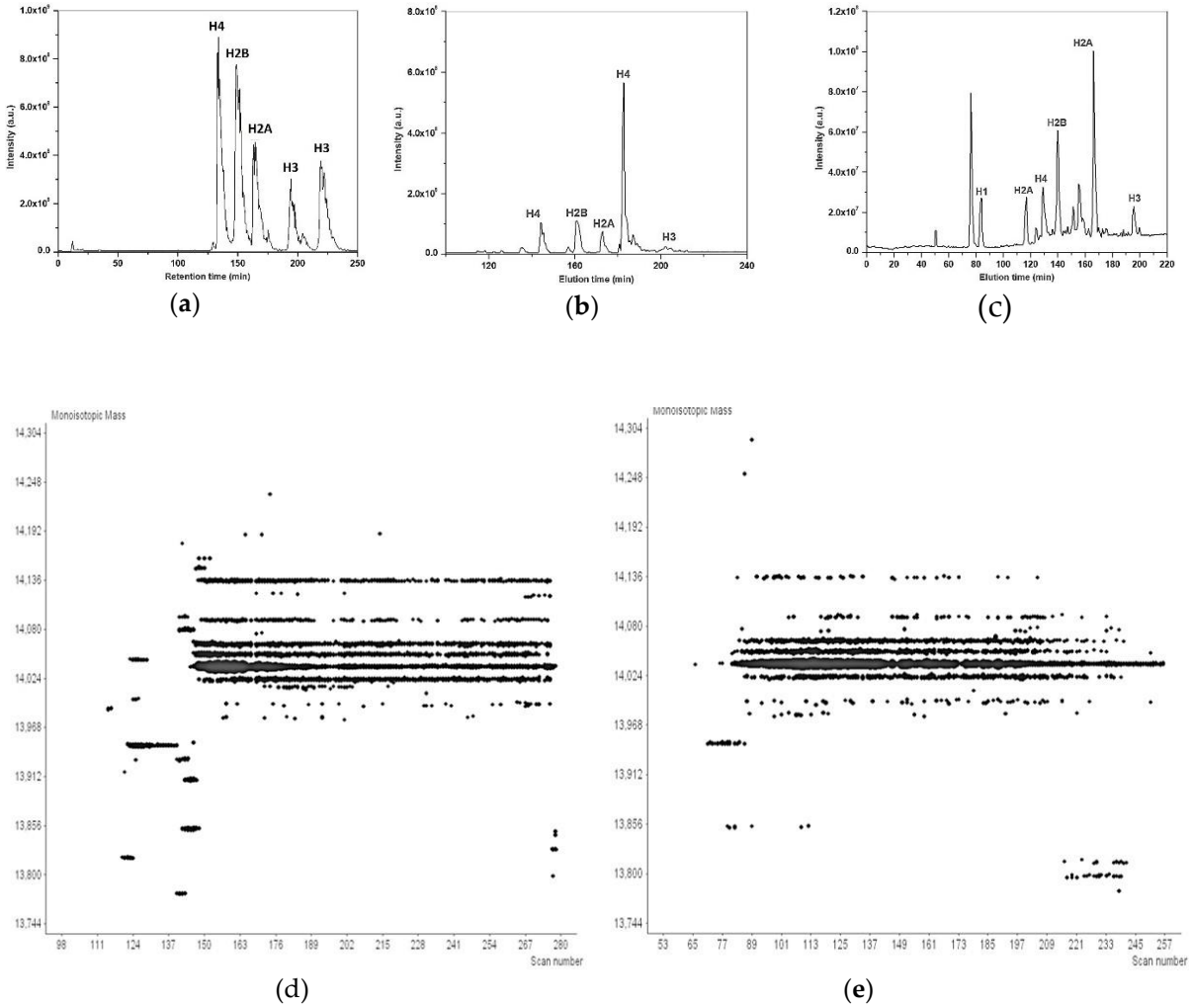

Figure 1. Representative mass spectral data of core histones from CD8+ T cells. (a-e) Mice were intranasally infected with influenza A virus strain A/X-31(H3N2) at EID_{50} of 10^6 and sacrificed on day 7. Spleens were harvested. CD8+ T cells were enriched, stained for surface markers, and sorted by FACS. Histones were purified and subjected to RPLC-MS/MS analysis on an Orbitrap Velos Mass Spectrometer. Mass spectra were acquired with high resolution to ensure isotopic resolution for all detected protein species. Representative data are provided for the total ion current of histones from HeLa cell standards (a), naïve CD8+ T cells (b) and activated CD8+ T cells (c). Two-dimensional displays depicting resolved intact protein masses of H2A from two independent experiments (d & e); species were detected using reversed-phase separation for activated T cells.

Due to the high degree of similarity between various histone isoform masses and the considerable difference in the amounts of each hore histone [Figure 1b & c], HiPTMap required extensive separation prior to detection in the mass spectrometer. We employed a combination of high-resolution protein separation and high-performance MS analysis for the identification of individual histone isomers. Raw data were then searched against mouse-specific anotated data to map top-down fragmentation spectral data to associated sequences for the identification of PTMs, including acetylation, mono-, di-, and trimethylation and phosphorylation [Supplemental File 1]. We identified 166 unique histone isoforms from naïve and activated CD8+ T cells isolated from the spleen of mice infected with influenza for 9 days [Table 1]. We validated the identity of these isoforms using online nanoflow WCX-HILIC LC-MS/MS (data not shown). WCX-HILIC MS/MS uses specialized separation for characterization of complex mixtures of hypermodified combinatorial proteins. However, WCX-HILIC only marginally increased the isoforms in the naïve T cells, so we continued with the RPLC-MS/MS-CID/ETD approach for HiPTMap.

 doi:10.20944/preprints202010.0215.v1

Table 1. Number of unique modified sequences identified from naïve and activated CD8+ T cells.

		H1F	H2A	H2B	H3	H4	Total
Naive	Identified		30	18	18	25	91
	Fragments		832	443	291	598	2164
	Unique Isoforms		9	6	16	19	50
Active	Identified	1	39	12	10	13	75
	Fragments	21	635	356	139	279	1430
	Unique Isoforms	1	10	5	9	12	36

The number of peptides identified, the sum of their corresponding fragments detected, and the total number of unique isoforms mapped.

Histones from naïve T cells had more total unique modified species than those from activated T cells [Table 1]. H2A was the only core histone with more unique modified sequences than those in naïve T cells (6 out of 9 contained lysine acetylation (K5ac)). This species was not present in H2A isolated from naïve mice. This trend remained true when K5ac was accompanied by serine 1 acetylation and/or threonine 120 phosphorylation (i.e., five found in activated T cells, one in naïve) [Table S1]. Core histones from H2B, H3, and H4 had more unique modified species detected in histones purified from naïve T cells [Table 1]. Lysine 108 acetylation was specific to H2B from naïve T cells [Table S1]. The peak intensity of H3 was lower than that of other core histones [Fig.1], resulting in low overall intensities for H3 isoforms from both naïve and activated T cells. However, H3 and H4 were generally more heavily modified, and these modifications were often associated with each other [Figure 2a and Table S1]. For example, lysine 9 through 36 on H3 were often acetylated and/or methylated in groups as were those on H4, whereas serine 1 acetylation was often accompanied by acetylation at positions 12 and 16 and methylation at position 20 [Figure 2 and Table S1]. In general, H4 had a relatively high level of triple and quadruple modifications that were distributed on a few amino acids [Figure 2a and Table S1]. One modification on H4 that was on twice as many unique sequences in naïve than in activated was serine 1 acetylation [Table S1]. Indeed, several of these species were not present in H4 histones from activated T cells (e.g., S1acK12acK16ac, S1acK12acK16acK20me3, S1acK16ac, S1acK16acK20me, S1acR3me2K20me3, and S1acR3meK20me2). However, some of these modifications were also detected exclusively in naïve histones from uninfected mice in the absence of serine 1 acetylation (e.g., K12acK16acK20me2 and K12acK16acK20me3). These findings indicate H3 and H4 are clad in multiple PTMs whose roles in T cell biology are currently unknown.

Preprints (www.preprints.org) | NOT PEER-REVIEWED | Posted: 12 October 2020 doi:10.20944/preprints202010.0215.v1

[Figure 2 about here]

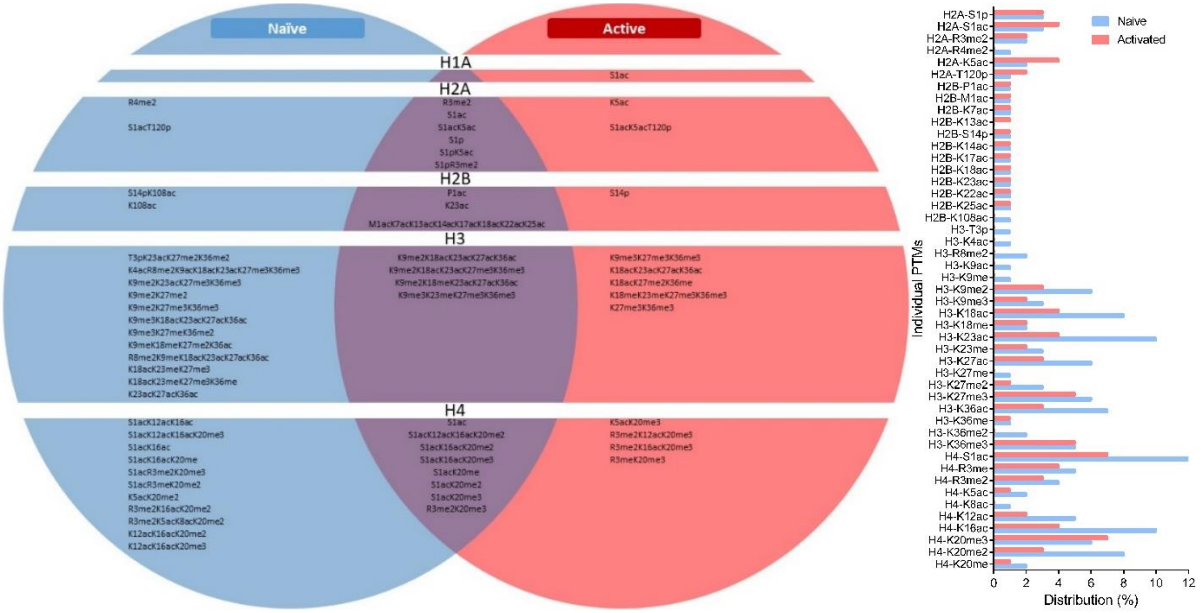

(a) (b)

Figure 2. HiPTMap of naïve and activated CD8 T cells. Histones purified from naïve ($CD8^{hi}$ $CD44^{low}$ $CD43^{low}$ $CD25^{low}$) or activated T cells ($CD8^{hi}$ $CD44^{hi}$ $CD43^{hi}$ $CD25^{hi}$) purified by FACS of splenocytes from mice 9 days after intranasal infection with influenza and subjected to RPLC-MS/MS-CID/ETD using Orbitrap Velos with alternative CID/ETD. Raw datasets were searched against Mouse – Top down database. PTMs including acetylation; mono-, di-, and tri-methylation; and phosphorylation were detected (a,b). The modifications for each proteoform were combined to yield the sum of each modification per core histone. A Wilcoxon matched-pairs signed-rank test was performed ($p < 0.0001$) with pairing evaluated by Spearman correlation ($p < 0.0001$).

To better compare proteoforms in naïve and activated T cells, we normalized one representative dataset with the total histone isoform intensities within the naïve and activated T cells [Table S2]. H2A accounted for the largest percentage of histone cores in activated T cells. We found acetylation of serine 1 on H2A (S1ac) was lower in relative intensity (i.e., 6.5% versus 23.4%) and in unique matched sequences in naïve versus activated T cells [Fig 2b and Table S2]. The relative abundance of peptides with phosphorylated serine 1 was also higher in activated T cells than in naïve (i.e., 21.3% versus 7.0%). Overall, H2B showed very few differences in counts or relative abundance within naïve or activated T cells. However, both the fragment numbers and peak intensity of acetylation of proline 1 were higher for H2B from activated T cells [Fig 2b and Table S1]. Interestingly, we identified four times more phosphorylated serine 14 H2B fragments from activated T cells than from naïve (i.e., 24 to 6). The relative abundance of H3 was the same irrespective of activation [Table S2]. H4 was the dominant species in the naïve T cells. Acetylation of serine 1 accounted for 38.1% of the isoforms detected in naïve and only 13.6% in activated T cells. Indeed, when we compared acetylation of the first twenty amino acids on H4, it encompassed 50.7% of all naïve species and 20.5% of all activated species identified. Apart from these exceptions, the majority of modified species we identified were present in histones from naïve and activated T cells to a similar extent [Table S1].

To determine if individual modifications changed following activation, we separated each individual PTM and compared the total number of each modifications per core histone [Fig 2b]. The distribution and median of PTMs per core histones from naïve and activated T cells were significantly different [Fig 2b]. H3K4 trimethylation is associated with increased transcriptional activity but was not detected in either subset. Six modifications were found in naïve but not in activated T cells: K108ac on H2B; T3p, K4ac, R8me2, and K9ac on H3; and K8ac on H4 [Fig 2b and Table S2]. Of these modifications, H3-K9ac and H4-K8ac are activators, and H3-R8me2 is associated with repression of gene expression [52-55]. Lysine 27 was also acetylated; this activation signal was detected twice as many times for naïve T cells than for activated (i.e., 108 versus 51

 doi:10.20944/preprints202010.0215.v1

fragments corresponding to 6 versus 3 unique species). Consistent with our previous finding [3], we found a reduction in the repressive mark lysine 27 di- and trimethylation associated with H3 from activated T cells [Fig 2b and Table S1]. There were 102 trimethylations detected on H3 from naïve T cells versus 68 from activated T cells [Table S1 & File S1A,B]. The same was true for dimethylations, with a total of 80 found in naïve and none on H3 from activated T cells. Single methylation of lysine 27 on H3 was detected 192 times in naïve versus 55 in activated T cells [Table S1 & File S1A,B]. Given trimethylation at lysine 27 is associated with repression of transcription of genes in these loci, these data are consistent with activation releasing repression at specific loci as opposed to increasing activation marks. Indeed, the only instances of more PTMs in activated T cells than in naïve were serine 1 and 5 acetylation of H2A [Fig 2b and Table S1].

3.2. Differences in activated T cell histone modification from the spleen, lung, and bronchial lavage

In the primary infection, influenza-specific CD8+ T cells expand and differentiate into effector cells that migrate to the respiratory tract and contribute to viral clearance [4]. We sought to determine if the relative abundance of histone modifications changed as T cells migrated to the site of infection. To accomplish this goal, we compared activated CD8+ T cells from the spleen, lung, and BAL removed from the same mice. The isoforms were grouped and intensities normalized across species for quantification [Supplemental File 2]. We found site one of histone H1F was acetylated in T cells from the lung and spleen to a similar extent [Fig 3A]. In constrast, we found ten modified forms of H2A [Fig 3B]. We detected the most modified fragments of acetylated serine one , which also had the highest intensity. Interestingly, serine 1 appeared to trend lower in both number and intensity as T cells migrated to infected tissue [Fig 3B]. The same held true for phosphorylation at serine 1. This PTM has been observed before and was associated with repression [56, 57]. Phosphorylation at serine 1 was accompanied by nearby dimethylation of arginine 3 and acetylation at lysine 5 that were

Preprints (www.preprints.org) | NOT PEER-REVIEWED | Posted: 12 October 2020 doi:10.20944/preprints202010.0215.v1

[Figure 3 about here]

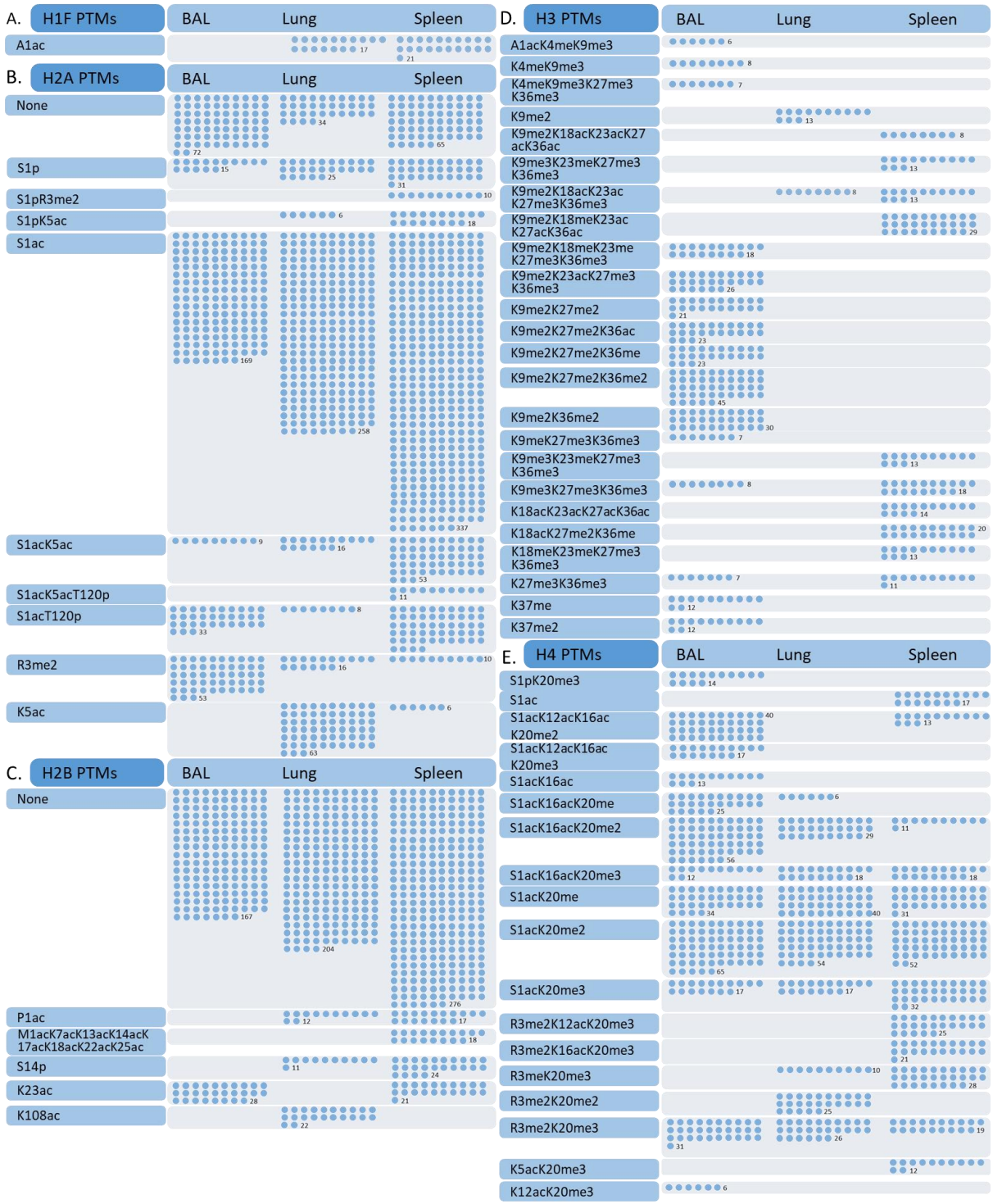

Figure 3. Distribution of modified species identified in histones purified from activated CD8+ T cells isolated from BAL, lung, and spleen after influenza infection. Activated T cells were isolated from BAL, lung, and spleen 9 days after influenza infection using FACS ($CD8^{hi}$ $CD44^{hi}$ $CD43^{hi}$ $CD25^{hi}$). Histones were purified from each sample, subjected to activated T cells purified by FACS of splenocytes from mice 9 days after intranasal infection with influenza, and subjected to RPLC-MS/MS-CID/ETD. Fragments identified per modified species (●) are indicated in score charts for H1F (A), H2A (B), H2B (C), H3 (D), and H4 (E).

highest in the spleen and absent in BAL [Fig 3B]. Demethylation of arginine appears to occur in combination with serine 1 phosphorylation, not acetylation. Surprisingly, arginine 3 demethylation of H2A was highly abundant in BAL, given when it was accompanied by serine 1 phosphorylation it was present in the spleen only. Lysine 5 acetylation was very high in the lung, both as a single modification

 doi:10.20944/preprints202010.0215.v1

and accompanying serine 1 acetylation [Fig 3B]. This combination is intriguing because this acetylation could block the repressive phosphorylation and acetylation of lysine 5 in mammals or 4 or 7 in *Saccharomyces cerevisiae*, which is associated with transcriptional activation [58-61]. These acetylation events were accompanied by phosphorylation at threonine 120, which is associated with promoting replication and gene expression changes associated with cancer [62], while others have shown it increases the genomic stability of replicating cells [63]. By contrast, H2B had fewer PTMs and the majority of species detected were unmodified, irrespective of T cell location [Fig 3C]. H2B phosphorylation at serine 14 (S14p) is considered an epigenetic marker of apoptotic cells that works in opposition to acetylation at the adjacent lysine 15 present in non-dying cells [64]. We detected some S14p in the spleen and lung [Fig 3E]. Lysine 23 acetylation was the only modification we detected on H2B in T cells from BAL, and lysine 108 acetylation was detected only on T cells from the lungs. Lysine 108 acetylation has been widely reported in other tissues and systems, but its function remains unknown [65-68].

H3 was heavily modified and studded with multiple modifications that were most abundant in the spleen and BAL [Fig 3D]. Of all the core histones, H3 exhibited a stark pattern of PTMs changing based on T cell location in BAL, lung, and spleen [Fig 3D]. Again, due to the lower relative abundance of H3, the normalized intensity of these isoforms was relatively low (i.e., ≤ 1%). However, these isoforms were detected many times. We did not detect trimethylation of lysine 4 (H3K4), the most well-known permissive mark. Nevertheless, this site was methylated and was present only in H3 from T cells in BAL [Fig 3D]. Notably, active genes are characterized by a combination of all three methylated forms of H3K4; mono- and dimethylation of H3K4 are found at both transcriptionally active promoters and distal regulatory elements and are considered activating signals [69-72]. We found repressive lysine 27 trimethylation on nine different isforms with many other PTMs [Fig 3D]. However, trimethylation at lysine 9 was present in 12 out of the 23 isoforms we confidently identified. Both H3K4me3 and H3K27me3 play an essential role in polarization and activation of immune cells, including CD8+ T cells [16, 17, 73-76]. Interestingly, we identified several species with lysine 9 (H3K9) methylations and H3K27 di- and trimethylations that were exclusively identified in BAL, expecially when PTMs were absent in the intervening region [Fig 3D]. This combination is also known for controlling the lineage commitment of T cells, including CD8+ T cells [77, 78]. Lysine 18 acetylation (K18ac) is also associated with transcription in T cell activation [17, 79]. H3K18 was almost exclusively found in T cells from the spleen. We also detected H3K37me in BAL. This species is noted in neuronal differentiation and cell adhesion but not in T cells. Thus, while H3 is of lower abundance, several modifications alone or in combination are associated with T cell activation and lineage commitment. Given the large number of PTMs surrounding known regulatory marks and the apparent enrichment of these species in different locations, exploring how these combinatorial patterns impact well-studied H3K4me3 and H3K27me3 may be worthwhile.

H4 was also heavily modified, and these modifications were clustered in the first twenty amino acids [Fig 3E]. The majority of these isoforms were detected at a similar frequency and relative intensity in BAL, lung, and spleen. The only exception was phosphorylation of serine 1 accompanied by trimethylation of lysine 20 [Fig 3E]. This S1pK20me3 isoform was found exclusively in BAL with several confidently matched fragments and was of high intensity (9%) [Fig 3E]. By contrast, phosphorylation of serine 1 on H2A was high in the spleen and diminished in BAL [Fig 3B]. Histone N-terminal tails contain high concentrations of acetylation and phosphorylation that alter the charge of the tails, thereby changing electrostatic interactions with chromatin. We detected phosphorylation of serine 1 on H4 (H4S1p), which has been implicated in the regulation of gene expression and control of cell phenotypes [80, 81] as well as decreasing histone acetyltransferase activity. We also detected dimethylation of arginine 3 (H4R3me2) that is capable of reversing the H4S1p effect, but we did not detect these PTMs in combination. We detected H4R3me2 in association with several other modifications, including K12 and K16 acetylation and K20 di- and trimethylation. These modifications tune complex binding and may play a role in enhancing or inhibiting regulatory complexes [82]. We also identified two other modifications, lysine 5 and 12 acetylation, associated with transcriptional

 doi:10.20944/preprints202010.0215.v1

activation [58-60]. Taken together, these analyses indicate a previously unappreciated role for histone modification dynamics in T cells during migration to local sites of infection.

3.3. Primary, memory, and secondary effector T cell histone modification

There are fundamental differences in the response of naïve versus educated T cells to infection. T cell expansion in response to primary infection lasts for 7-10 days and is followed by contraction, leaving 5-10% of antigen-specific CD8+ T cells to form the pool of memory cells. In a subsequent "secondary" infection, these cells expand more robustly and mediate viral clearance faster. We compared the histones from activated CD8+ T cells from the peak of the primary response (day 9) to early effector–memory cells (day 30) and to activated T cells collected 7 days following a heterologous challenge. All mice were intranasally infected with influenza strain X31. However, for the secondary condition, mice were infected with a different strain of influenza (PR8) at least 30 days prior to infection with strain X31. Supplementary files 2B, C and D contains the complete list of observed species, their masses, and p-values for primary, memory, and secondary, respectively. We compared the invidual PTMs per condition [Fig 4]. Primary and memory were not significantly different, while secondary had signficantly more modifications than primary or memory [Fig4a]. Interestingly, acetylation of lysine 5, a transcriptional activation mark on H2A [59, 60], was similar for all groups [Fig 4a and Table 3]. Dimethylation of arginine 4 and acetylation of lysine 13 are known to target this area for biotinylation, which is involved in cell proliferation [83, 84]. H2AR4me2 and H2AK13ac were detected only in the secondary response [Fig 4a and Table 2]. Apart from H2AR4me2 and H2AK13sc, H2A appears to have similar modifications irrespective of the T cell state [Fig 2b and 4a]. [Table 2 about here]

Table 2. H2A modifications in T cells from primary, memory, and secondary responses.

H2A	Primary		Memory		Secondary	
	Peptides	Detected	Peptides	Detected	Peptides	Detected
S1ac	15	377	21	304	26	749
S1p	2	31	2	26	4	75
R3me2	1	10	1	1	3	13
R4me2					1	20
K5ac	6	6	6	6	5	5
S1acK5ac	4	53	2	59	5	95
S1acR3me2K5ac					2	21
S1acK5acT120p	1	11				
S1acT120p	4	54	1	1	5	98
S1pK5ac	2	18				
S1pR3me2	1	10	1	9	3	74
K13ac					1	12
None	2	65	5	155	8	158

Peptides: the number of unique peptides identified containing modification. Detected: the sum of the fragments detected.

[Figure 4 about here]

Preprints (www.preprints.org) | NOT PEER-REVIEWED | Posted: 12 October 2020 doi:10.20944/preprints202010.0215.v1

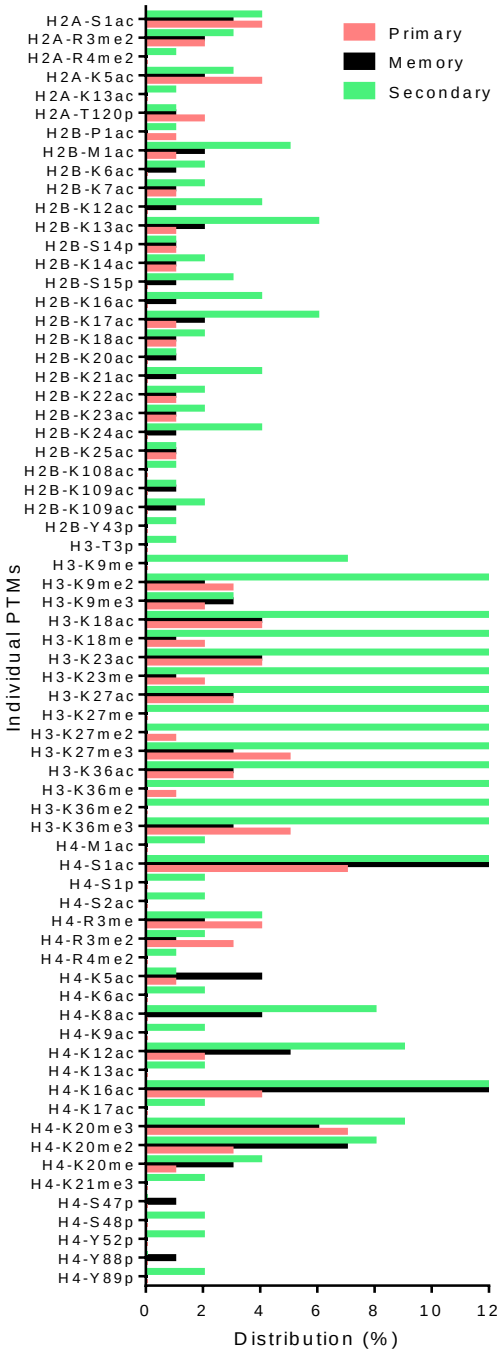

(a)

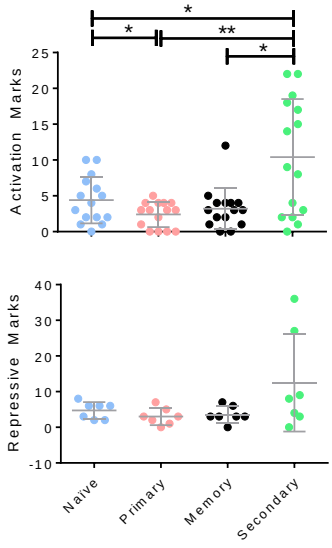

(b)

Figure 4. HiPTMapping of primary, memory, and secondary CD8+ T cells. Activated T cells ($CD8^{hi}$ $CD44^{hi}$ $CD43^{hii}$) were isolated by FACS after primary and secondary infections along with effector memory cells ($CD8^{hi}$ $CD44^{+}$ $CD43^{+}$). Spleens were harvested 9, ≥30, or 7 days after intranasal infection with influenza for primary, memory, and secondary responses, respectively. In the secondary response, mice were infected with influenza strain PR8 at least 30 days prior to infection with strain X31. Prior to sorting, contaminated immune cells were reduced by negative depletion. Histones were purified from T cells and subjected to RPLC-MS/MS using Orbitrap Velos with alternative CID/ETD. Raw datasets were searched against the Mouse–Top down database. PTMs including acetylation; mono-, di-, and trimethylation; and phosphorylation were detected. The occurence of each modification per proteoform was combined to yield the sum of each specific PTM per core histone (a,b). ANOVA ($p < 0.0001$) was performed followed by Tukey's multiple comparisons test: Primary -vs- Memory ($p=0.3291$), Memory -vs- Secondary (<0.0001), and Primary -vs- Secondary ($p < 0.0001$) (a). PTMs were separated into known activation marks (H2A-S1p, H2A-K5ac, H3-K36me2, H3-K9ac, H3-K27ac, H2B-K12ac, H3-K18ac, H3-K23ac, H3-K36ac , H3-K36me3, H4-K5ac, H4-K8ac, H4-K12ac, H4-K8ac, H4-R3me2, and H4-K16ac) and repressive marks (H3-R8me2, H3-K9me2, H3-K9me3, H3-K27me3, H4-K20me2, H4-K20me3, H4-K20me). The naïve T cells *($CD8^{hi}$ $CD44^{low}$ $CD43^{low}$ $CD25^{low}$)* that were isolated in primary infections were also compared. ANOVA ($p = 0.007$) followed by Tukey's multiple comparisons test [$p < 0.05$ (*) and $p < 0.005$ (**)] (b).

When we compared modifications to H2B, we found T cells in the secondary response showed a high distribution of almost all proteoforms identified [Table 2 and Fig 4]. We identified P1ac on the H2B1C isoform in the primary infection. When accompanied by a string of acetylations in this region, P1ac was found in the secondary response. In constrast, acetylations at residues 16, 17, 18, 22, and 24 were present in all three groups. Acetylations at lysine 7, 12, 13, and 14 were largely associated with the secondary response [Fig 4 and Table 3]. The addition of phosphorylation at tyrosine 43 on H2B occurred only in the secondary response [Table 3]. Phosphorylation of serine 14 (S14p) in the absence

Preprints (www.preprints.org) | NOT PEER-REVIEWED | Posted: 12 October 2020 doi:10.20944/preprints202010.0215.v1

of H2AXphosphorylation is highly correlated with somatic hypermutation *in vivo* and class switch recombination [85]. We found no evidence of H2AX phosphorylation with consistent S14p across all three groups [Fig 4 and Table 2]. Lysine 20 was acetylated in memory and secondary responses [Table 3]. This modification was previously detected on H2B [86] and was recently implicated as the site-specific homing and docking point for macroH2A1, which is required for the transcriptional activation of a myriad of cytokines, chemokines, metalloproteases [87]. Acetylation at the tail region was not present in the primary response (e.g., lysine 108 or 109).

Table 3. H2B modifications in T cells from primary, memory, and secondary responses.

H2B	Primary		Memory		Secondary	
Species	Peptides	Detected	Peptides	Detected	Peptides	Detected
P1ac	1	17				
P1acK6acK12acK13acK16acK17acK21acK24acK109ac					1	15
M1acK6acK12acK13acS15pK16acK17acK21acK24acY43p					2	59
M1acK7acK13acK14acK17acK18acK22ac					1	23
M1acK7acK13acK14acK17acK18acK22acK25ac	1	18	1	24	2	56
M1acK12acK13acS15pK16acK17acK21acK24ac					1	28
M1acK12acK13acS15pK16acK17acK21acK24acK109ac			1	15	1	16
S14p	1	24	2	35	5	135
K20acK23ac			3	31	8	310
K23ac	1	21			7	259
K108ac					2	83
None	8	267	10	286	22	804

Peptides: the number of unique peptides identified containing modification. Detected: the sum of the fragments detected.

Despite loading the same amount of histones, we found very few H3 isoforms in the memory sample [Table 4 and File S1C]. We did not find any methylation at lysine 4, a permissive mark. However, we found repressive methylation of lysine 9 and 27. These modifications were in the same peptides three times in the primary sample and twelve times in the secondary. We also found a similar level of acetylation of lysine 27, an enhancer signal [88]. We detected lysine 36 acetylation and methylation, which are promoter marks on activated and repressed genes, respectively [89]. The acetylation to methylation ratios were 3 to 6 for the primary sample and 18 to 22 for the secondary. The relative ratios were not significantly different for these events. The most striking differences in individual modifications on H3 were observed in regions 9 to 37 [Fig 4a]. This area contains seven known activators (K4ac, K9me, K18ac, K23ac, K36me, and K37me) [58, 60, 90-95] and and three repressor signals (R8me, K9me, and K27me) [96-100]. This region is heavily modified with many combinations of methylations and acetylations [Table 4]. In some cases, these modifications represent opposing signals on a single amino acid, such as acetylation or methylation of lysine 9 inducing activation or repression at nearby loci [101, 102]. There were also bivalent marks at neighboring sites such as methylation of lysine 36 and 37, which are activation and repression marks, respectively [101, 102]. The abundance of H3 species with activation and repression marks indicates these histones may be poised to respond to external condition changes in these states.

Table 4. H3 modifications in T cells from primary, memory, and secondary responses.

H3	Primary		Memory		Secondary	
Species	Identified	Detected	Identified	Detected	Identified	Detected
T3pK9me3K27me3K36me					1	11
R8me2K9meK18acK23acK27acK36ac			1	10		
K9me2K18me					1	29
K9meK18meK23meK27me					1	32
K9meK18meK23meK27meK36me			1	10	2	58
K9me2K18meK27me					1	27
K9meK18meK27me2K36me					4	124
K9me2K18meK36me3					1	22
K9me2K18meK23acK27acK36ac	2	29			1	28
K9meK18meK27meK36ac					2	61
K9meK18acK23acK27acK36ac	1	8	2	26		
K9me2K18acK23acK27me3K36me3	1	13	1	9	1	25
K9me2K18acK36ac					1	24
K9me2K23meK27me					2	58
K9meK23meK27meK36me	1	13			4	98
K9me2K23meK36me3					1	26
K9me2K23meK27meK36ac					1	31
K9me2K23acK27acK36ac					1	24
K9me2K23acK27me3K36me3					2	47

 doi:10.20944/preprints202010.0215.v1

K9me3K23acK27acK36me3					1	24
K9me2K27me					6	168
K9meK27meK36me	1	18	1	7	17	501
K9me2K27ac					2	53
K9me2K27acK36me					2	47
K9me2K27acK36ac					1	29
K9me2K27me2K36ac					3	76
K9me2K36ac					3	77
K9me2K36me					4	110
K18meK23meK27me3K36me3	1	13			1	26
K18acK23meK27me3K36me					2	49
K18acK23acK27acK36ac	1	14			1	23
K18acK23meK27acK36ac					2	56
K18acK23acK27meK36ac					1	26
K18acK23acK27meK36me					4	109
K18acK23meK27me2K36ac					1	22
K18acK23meK27me3					1	32
K18meK27me3K36me3					1	16
K18acK27acK36ac					2	52
K18acK27acK36me					4	100
K18acK27meK36me	1	20			2	61
K18acK27meK36ac					2	48
K23meK27me3					3	72
K23meK27me3K36me					7	185
K23meK27meK36ac					2	60
K23acK27me					1	31
K23acK27me3K36ac					1	22
K23acK27meK36me					4	107
K27acK36ac					5	137
K27acK36me					4	119
K27me2					1	30
K27meK36me	1	11			10	268
K27meK36ac					3	89

Peptides: the number of unique peptides identified containing modification. Detected: the sum of the fragments detected. Underline indicates mono, di, and trimethylation were combined.

H4 had fewer unique combinations of modifications than H3, but most H4 proteoforms were detected within the memory group [Table 5]. Serine 1 was acetylated in all groups and phosphorylated in the secondary response. This phosphorylation event is associated with proliferation [56]. Arginine 3 methylation (R3me) is a permissive mark [93, 103, 104] that we found in combination with serine 1 phosphorylation in the secondary response [Table 5]. R3me was present in both primary and secondary responses on multiple H4 peptides in combination with other activators and the repressive mark K20me [90, 105-107]. Acetylations at lysine 5 or 8 are also activation marks [58-60, 108-110] and were associated with both primary and secondary responses [Table 5]. Acetylations of nearby lysine 12 and 16 are also activation marks [58-60, 108, 109, 111]; these marks were present in all states but had much higher distributions in memory and secondary T cells [Fig 4a]. Acetylation of lysine 9 is also an activation mark [52, 53], but it was detected only in the secondary response [Fig4a]. Similar to H2, acetylations were grouped closely together in this region. Interestingly, K16ac was often accompanied by K20me. This repressive mark was on approximately 50% of the secondary species we identified and 75-88% of the species in the primary and memory groups. In contrast to H3 where we found an abundance of species with activation and repression marks, all H4 PTMs with known functions were associated with transcriptional activation except for monomethylation of lysine 20, which has been associated with both activation [90] and repression [105-107].

Preprints (www.preprints.org) | NOT PEER-REVIEWED | Posted: 12 October 2020 doi:10.20944/preprints202010.0215.v1

Table 5. H4 modifications in T cells from primary, memory, and secondary responses.

H4	Primary		Memory		Secondary	
Species	Identified	Detected	Identified	Detected	Identified	Detected
S1ac	1	17			1	15
S1pR3me					1	6
S1pR3meK20me3					2	23
S1acR3meK20me2			1	14		
S1acK5acK8acK12acK16ac					2	22
S1acK5acK8acK12acK16ac			1	19		
S1acK5acK8acK12acK16acK20me2			1	13		
S1acK5acK8acK16acK20me			1	23		
S1acK5acK12acK16acK20me			1	27		
S1acK8acK12acK16ac					2	43
S1acK8acK12acK16acK20me			1	56	3	48
S1acK8acK16acK20me					5	135
S1acK12acK16ac					3	69
S1acK12acK16acK20me	1	13	2	78	7	202
S1acK16ac			1	12	4	79
S1acK16acK20me	2	29	5	191	10	301
S1acK16acK20me3S47p			1	9		
S1acK20me	4	115	6	241	9	266
S1acK20me3Y88p			1	19		
R3me2K12acK20me3	1	25				
R3me2K16acK20me	1	21			1	10
R3meK20me	2	47	1	23	2	25
K5acK20me3	1	12				
K16ac			1	13		
K16acK20me					2	31
K20me			2	97	2	34
M1acS2acK6acK9acK13acK17acK21me3-S48pY52pY89p					1	6
M1acS2acR4me2K6acK9acK13acK17ac-K21me3S48pY52pY89p					1	6
None					2	24

Peptides: the number of unique peptides identified containing modification. Detected: the sum of the fragments detected. Underline indicates mono, di, and trimethylation were combined.

4. Discussion

Histone modifications in the respiratory tract have been associated with respiratory inflammation and infection. Some histone mark distributions were uniquely associated with the transcription rates of genes. For example, H3K9me3 and H3K27me3 levels at the COX2 promoter were substantially higher in primary human lung fibroblasts isolated from patients with idiopathic pulmonary fibrosis [112] and have been reported in lung tissue during SARS-CoV infection [113]. Likewise, epigenetic changes by influenza may alter the host response. Alterations in DNA methylation reportedly occur in promoter regions of some proinflammatory cytokines and interleukin genes in response to influenza infection [114-116]. Influenza infection can also modulate PTMs [117, 118]. While these studies focused on specific canonical regulation markers, they suggested highly pathogenic avian H5N1 influenza infection induces PTMs distinct from those induced by the H1N1 2009 pandemic strain [117, 118]. This difference is likely due to the influenza infection complex, which is composed of non-structural and polymerase viral proteins and host chromatin remodeler proteins and functions to induce modifications that specifically remodel chromatin [119-121]. Thus, although influenza virus does not integrate into the host genome, active transport of viral proteins into the nucleus that facilitate early stage transcription and replication occurs and may mediate previously observed epigenetic changes in lung tissue. However, T cells are not a major source of influenza replication. Thus, the distinct epigenetic maps of T cells we observed in the various T cell states following influenza infection were more likely due to T cell activation and lineage.

Previous studies have profiled H3K4me3 and H3K27me3 at certain effector gene loci of T cell subsets and determined these marks are associated with specific genes that are critical to functions related to these phenotypes [122, 123]. Genome-wide ChIP-Seq was used to determine gene expression profiles in human naive and memory CD8(+) T cells associated with these modifications and found correlations between gene expression and the amounts of H3K4me3 (positive correlation) and H3K27me3 (negative correlation) across the gene body [17]. Araki and co-workers found memory T cells have more genes with high levels of H3K4me3 marks than naïve cells and defined 4 associations between these two modifications and gene expression with the T cell state. Resting memory T cells have repressed genes (i.e., high H3K27me3 and low H3K4me3 with low mRNA expression) as well as

 doi:10.20944/preprints202010.0215.v1

active and poised genes (i.e., low H3K27me3 and high H3K4me3 with either high or low mRNA expression, respectively) [17]. The fourth group, termed bivalent, maintained low mRNA expression in naïve and resting memory cells with strikingly increased expression upon activation of memory T cells in association with high levels of both H3K27me3 and H3K4me3 [17]. A similar approach was used to demonstrate naïve T cells maintain bivalency at gene loci that regulate transcription, replication, and cellular differentiation; however, after *in vivo* differentiation into influenza-specific effector T cells, the transcriptional silencing marks were lost [3]. Russ et al also demonstrated this was distinct from immune-related effector gene promoters that acquired permissive H3K4me3 modification after activation [3]. We used an unbiased approach and did not identify H3K4me3 or mine the data and attempt to resolve or quantify this species. However, we found a reduction in the repressive mark lysine 27 di- and trimethylation associated with H3 with T cell activation [Fig 2b and Table S1]. We identified more unique combinations of PTMs from naïve than activated T cells isolated from the same samples, as well as significantly more individual PTMs and known markers of transcriptional activation. Moreover, after a secondary recall response to heterologous influenza challenge, activation of effector memory T cells significantly increased the number of PTMs known to mediate transcriptional activation compared to naïve, primary, or memory effector T cells. This was largely due to several internal acetylations of lysine 9, 18, 23, 27 and 36 on H3. Internal lysine acetylations on histones are generally associated with transcriptional activation via charge neutralization relaxing the chromatin structure to open transcription in the region [124, 125]. This was complemented by di- and trimethylation at lysine 36, a strong enhancer of transcriptional activation in T cells. Indeed, increased chromatin accessibility via hyperacetylation of this region is a potentially important mechanism for rapid re-expression of effector genes that facilitates the unique capacity for rapid recall of effector CD8+ T cells [126].

Araki and Russ et al. established that H3K4me3 and H3K27me3 are reliably associated with genes that regulate T cell differentiation and function. Deposition of H3K4me3 and H3K27me3 correlate with the expression patterns of many critical genes, and these positive and negative correlations, respectively, are consistent with T cell phenotypes and their functions. Moreover, the methylation levels of lysine 4 and 27 on H3 change dynamically during an immune response, and memory T cells are characterized by both PTMs, making these loci poised for rapid expression. Our findings add to this knowledge by defining new PTM combinations and mapping these epigenetic hot spots on histones in distinct CD8+ T cell subsets. Similar to the canonical H3K4me3 and H3K27me3 modifications detailed above, we found many proteoforms that were bivalent in effector T cell subsets. Furthermore, there were significant distribution differences in histone PTMs from CD8+ T cells recalled to activation from secondary heterologous influenza infection. Recent research in this area suggests that even minor changes in highly conserved regions alter chromatin structure and gene regulation [127, 128]. Due to their high heterogeneity, histones are inherently challenging to study; additionally, interpreting combinations of histone marks is difficult because of the lack of knowledge regarding their biological function [129-131]. However, our identification of these differentially marked histones in unique combinations from distinct T cell subsets raises several important questions. First, are these histone PTMs integral to controlling gene expression in the T cell response or do they play other currently undefined roles? If the former is true, PTMs may act to fine tune canonical modifications or function independently. Second, are the acetylations on H4 from lysine 6 to 17 that are associated with memory and secondary T cell subsets mediating memory cell survival or homeostatic proliferation upon recall? HiPTMap of T cells acquired *ex vivo* from the same groups of mice (e.g., activated versus naïve T cells or effector T cells from different compartments) as well as identifying PTMs across effector T cells (primary, memory, and secondary) has provided the blueprint to answer some of these questions and will likely contribute to our understanding of epigenetic regulation of T cell biology.

5. Conclusions

The HiPTMap strategy used here enhances data quality and acquisition sensitivity, providing comprehensive analysis. Our results show the high potential of online nanoflow 2DLC separation using two orthogonal separation modalities for top-down analysis of histones. Both methods were

online coupled and eluted at a nanoflow rate to reduce sample dilution and enhance MS sensitivity. In addition, this platform extended the dynamic range of MS measurements, increasing the number of confidently identified histone proteoforms compared to 1DLC-MS. With this strategy, we identified hundreds of unique histone-modified species isolated directly *ex vivo* following influenza infection. As a result, we now know that several new bivalent combinations are present in effector T cells, the histone map changes as T cells relocate during influenza infection, and the secondary recall response of CD8+ T cells induces a significant increase in histone PTMs associated with transcriptional activation.

Supplementary Materials: The following are available online at www.mdpi.com/xxx/s1, Table S1: Modified core histone species identified in naive and activated CD8+ T cells. Table S1: Relative abundance of histone modifications from naïve and activated CD8+ T-cells. File S1: Summary MS data of T cell subsets after primary and secondary influenza infection. File S2: Summary MS data of histones from activated CD8 T cells from the spleen, BAL, and lung after influenza infection.

Author Contributions Conceptualization, Ljiljana Pasa-Tolic and Heather S. Smallwood; Data curation, Svetlana Rezinciuc, Zhixin Tian, Sisi Wu and Shawna Hengel; Formal analysis, Nikola Tolić, Zhixin Tian, Sisi Wu and Shawna Hengel; Investigation, Heather S. Smallwood; Methodology, Nikola Tolić, Zhixin Tian and Ljiljana Pasa-Tolic; Project administration, Ljiljana Pasa-Tolic; Resources, Ljiljana Pasa-Tolic and Heather S. Smallwood; Software, Nikola Tolić; Supervision, Heather S. Smallwood; Validation, Sisi Wu and Shawna Hengel; Writing – original draft, Svetlana Rezinciuc and Heather S. Smallwood; Writing – review & editing, Svetlana Rezinciuc, Ljiljana Pasa-Tolic and Heather S. Smallwood.

Funding: This research was funded by the Le Bonheur Young Investigator Award and the Children's Foundation Research Institute, Memphis, Tennessee, USA (H.S.S.).

Acknowledgments: The authors wish to thank Matthew E. Monroe of Pacific Northwest National Laboratory for assembling these data and Courtney Bricker-Anthony of the Children's Foundation Research Institute for scientific editing.

Conflicts of Interest: The authors declare no conflict of interest. The funders had no role in the design of the study; in the collection, analyses, or interpretation of data; in the writing of the manuscript, or in the decision to publish the results.

References

1. Turner SJ, Kedzierska K, La Gruta NL, Webby R, Doherty PC. Characterization of CD8+ T cell repertoire diversity and persistence in the influenza A virus model of localized, transient infection. Seminars in immunology. 2004;16(3):179-84. Epub 2004/05/08. doi: 10.1016/j.smim.2004.02.005. PubMed PMID: 15130502.

2. La Gruta NL, Turner SJ, Doherty PC. Hierarchies in cytokine expression profiles for acute and resolving influenza virus-specific CD8+ T cell responses: correlation of cytokine profile and TCR avidity. Journal of immunology. 2004;172(9):5553-60. Epub 2004/04/22. doi: 10.4049/jimmunol.172.9.5553. PubMed PMID: 15100298.

3. Russ BE, Olshanksy M, Smallwood HS, Li J, Denton AE, Prier JE, et al. Distinct epigenetic signatures delineate transcriptional programs during virus-specific CD8(+) T cell differentiation. Immunity. 2014;41(5):853-65. Epub 2014/12/18. doi: 10.1016/j.immuni.2014.11.001. PubMed PMID: 25517617; PubMed Central PMCID: PMCPMC4479393.

4. Duan S, Thomas PG. Balancing Immune Protection and Immune Pathology by CD8(+) T-Cell Responses to Influenza Infection. Frontiers in immunology. 2016;7:25. Epub 2016/02/24. doi: 10.3389/fimmu.2016.00025. PubMed PMID: 26904022; PubMed Central PMCID: PMCPMC4742794.

5. Duan S, Meliopoulos VA, McClaren JL, Guo XZ, Sanders CJ, Smallwood HS, et al. Diverse heterologous primary infections radically alter immunodominance hierarchies and clinical outcomes following H7N9 influenza

challenge in mice. PLoS pathogens. 2015;11(2):e1004642. Epub 2015/02/11. doi: 10.1371/journal.ppat.1004642. PubMed PMID: 25668410; PubMed Central PMCID: PMCPMC4335497.

6. Kannan A, Huang W, Huang F, August A. Signal transduction via the T cell antigen receptor in naive and effector/memory T cells. Int J Biochem Cell Biol. 2012;44(12):2129-34. Epub 2012/09/18. doi: 10.1016/j.biocel.2012.08.023. PubMed PMID: 22981631; PubMed Central PMCID: PMCPMC3532926.

7. Ghoneim HE, Fan Y, Moustaki A, Abdelsamed HA, Dash P, Dogra P, et al. De Novo Epigenetic Programs Inhibit PD-1 Blockade-Mediated T Cell Rejuvenation. Cell. 2017;170(1):142-57 e19. Epub 2017/06/27. doi: 10.1016/j.cell.2017.06.007. PubMed PMID: 28648661; PubMed Central PMCID: PMCPMC5568784.

8. Abdelsamed HA, Zebley CC, Youngblood B. Epigenetic Maintenance of Acquired Gene Expression Programs during Memory CD8 T Cell Homeostasis. Frontiers in immunology. 2018;9:6. Epub 2018/02/07. doi: 10.3389/fimmu.2018.00006. PubMed PMID: 29403491; PubMed Central PMCID: PMCPMC5778141.

9. Youngblood B, Noto A, Porichis F, Akondy RS, Ndhlovu ZM, Austin JW, et al. Cutting edge: Prolonged exposure to HIV reinforces a poised epigenetic program for PD-1 expression in virus-specific CD8 T cells. Journal of immunology. 2013;191(2):540-4. Epub 2013/06/19. doi: 10.4049/jimmunol.1203161. PubMed PMID: 23772031; PubMed Central PMCID: PMCPMC3702641.

10. Harland KL, Day EB, Apte SH, Russ BE, Doherty PC, Turner SJ, et al. Epigenetic plasticity of Cd8a locus during CD8(+) T-cell development and effector differentiation and reprogramming. Nature communications. 2014;5:3547. Epub 2014/03/29. doi: 10.1038/ncomms4547. PubMed PMID: 24675400; PubMed Central PMCID: PMCPMC3974221.

11. Denton AE, Russ BE, Doherty PC, Rao S, Turner SJ. Differentiation-dependent functional and epigenetic landscapes for cytokine genes in virus-specific CD8+ T cells. Proceedings of the National Academy of Sciences of the United States of America. 2011;108(37):15306-11. Epub 2011/08/31. doi: 10.1073/pnas.1112520108. PubMed PMID: 21876173; PubMed Central PMCID: PMCPMC3174616.

12. Juelich T, Sutcliffe EL, Denton A, He Y, Doherty PC, Parish CR, et al. Interplay between chromatin remodeling and epigenetic changes during lineage-specific commitment to granzyme B expression. Journal of immunology. 2009;183(11):7063-72. Epub 2009/11/17. doi: 10.4049/jimmunol.0901522. PubMed PMID: 19915065.

13. Allan RS, Zueva E, Cammas F, Schreiber HA, Masson V, Belz GT, et al. An epigenetic silencing pathway controlling T helper 2 cell lineage commitment. Nature. 2012;487(7406):249-53. Epub 2012/07/06. doi: 10.1038/nature11173. PubMed PMID: 22763435.

14. Seumois G, Chavez L, Gerasimova A, Lienhard M, Omran N, Kalinke L, et al. Epigenomic analysis of primary human T cells reveals enhancers associated with TH2 memory cell differentiation and asthma susceptibility. Nature immunology. 2014;15(8):777-88. Epub 2014/07/07. doi: 10.1038/ni.2937. PubMed PMID: 24997565; PubMed Central PMCID: PMCPMC4140783.

15. Ansel KM, Djuretic I, Tanasa B, Rao A. Regulation of Th2 differentiation and Il4 locus accessibility. Annu Rev Immunol. 2006;24:607-56. Epub 2006/03/23. doi: 10.1146/annurev.immunol.23.021704.115821. PubMed PMID: 16551261.

16. Wei G, Wei L, Zhu J, Zang C, Hu-Li J, Yao Z, et al. Global mapping of H3K4me3 and H3K27me3 reveals specificity and plasticity in lineage fate determination of differentiating CD4+ T cells. Immunity. 2009;30(1):155-67. Epub 2009/01/16. doi: 10.1016/j.immuni.2008.12.009. PubMed PMID: 19144320; PubMed Central PMCID: PMCPMC2722509.

17. Araki Y, Wang Z, Zang C, Wood WH, 3rd, Schones D, Cui K, et al. Genome-wide analysis of histone methylation reveals chromatin state-based regulation of gene transcription and function of memory CD8+ T cells.

Immunity. 2009;30(6):912-25. Epub 2009/06/16. doi: 10.1016/j.immuni.2009.05.006. PubMed PMID: 19523850; PubMed Central PMCID: PMCPMC2709841.

18. Veiga-Fernandes H, Walter U, Bourgeois C, McLean A, Rocha B. Response of naive and memory CD8+ T cells to antigen stimulation in vivo. Nature immunology. 2000;1(1):47-53. Epub 2001/03/23. doi: 10.1038/76907. PubMed PMID: 10881174.

19. Kaech SM, Hemby S, Kersh E, Ahmed R. Molecular and functional profiling of memory CD8 T cell differentiation. Cell. 2002;111(6):837-51. Epub 2003/01/16. doi: 10.1016/s0092-8674(02)01139-x. PubMed PMID: 12526810.

20. Pizzolla A, Nguyen TH, Sant S, Jaffar J, Loudovaris T, Mannering SI, et al. Influenza-specific lung-resident memory T cells are proliferative and polyfunctional and maintain diverse TCR profiles. The Journal of clinical investigation. 2018;128(2):721-33. Epub 2018/01/09. doi: 10.1172/JCI96957. PubMed PMID: 29309047; PubMed Central PMCID: PMCPMC5785253.

21. Andreansky SS, Stambas J, Thomas PG, Xie W, Webby RJ, Doherty PC. Consequences of immunodominant epitope deletion for minor influenza virus-specific CD8+-T-cell responses. Journal of virology. 2005;79(7):4329-39. Epub 2005/03/16. doi: 10.1128/JVI.79.7.4329-4339.2005. PubMed PMID: 15767433; PubMed Central PMCID: PMCPMC1061524.

22. Keating R, Morris MY, Yue W, Reynolds CE, Harris TL, Brown SA, et al. Potential killers exposed: tracking endogenous influenza-specific CD8(+) T cells. Immunology and cell biology. 2018;96(10):1104-19. Epub 2018/07/05. doi: 10.1111/imcb.12189. PubMed PMID: 29972699; PubMed Central PMCID: PMCPMC6282960.

23. Souquette A, Thomas PG. Past Life and Future Effects-How Heterologous Infections Alter Immunity to Influenza Viruses. Frontiers in immunology. 2018;9:1071. Epub 2018/06/07. doi: 10.3389/fimmu.2018.01071. PubMed PMID: 29872429; PubMed Central PMCID: PMCPMC5972221.

24. Wu JI, Lessard J, Crabtree GR. Understanding the words of chromatin regulation. Cell. 2009;136(2):200-6. Epub 2009/01/27. doi: 10.1016/j.cell.2009.01.009. PubMed PMID: 19167321; PubMed Central PMCID: PMCPMC2770578.

25. Kelly TK, De Carvalho DD, Jones PA. Epigenetic modifications as therapeutic targets. Nature biotechnology. 2010;28(10):1069-78. Epub 2010/10/15. doi: 10.1038/nbt.1678. PubMed PMID: 20944599; PubMed Central PMCID: PMCPMC3022972.

26. Sadakierska-Chudy A, Filip M. A comprehensive view of the epigenetic landscape. Part II: Histone post-translational modification, nucleosome level, and chromatin regulation by ncRNAs. Neurotox Res. 2015;27(2):172-97. Epub 2014/12/18. doi: 10.1007/s12640-014-9508-6. PubMed PMID: 25516120; PubMed Central PMCID: PMCPMC4300421.

27. Burgess RJ, Zhang Z. Histone chaperones in nucleosome assembly and human disease. Nat Struct Mol Biol. 2013;20(1):14-22. Epub 2013/01/05. doi: 10.1038/nsmb.2461. PubMed PMID: 23288364; PubMed Central PMCID: PMCPMC4004355.

28. Eberharter A, Becker PB. Histone acetylation: a switch between repressive and permissive chromatin. Second in review series on chromatin dynamics. EMBO Rep. 2002;3(3):224-9. Epub 2002/03/08. doi: 10.1093/embo-reports/kvf053. PubMed PMID: 11882541; PubMed Central PMCID: PMCPMC1084017.

29. Stengel KR, Zhao Y, Klus NJ, Kaiser JF, Gordy LE, Joyce S, et al. Histone Deacetylase 3 Is Required for Efficient T Cell Development. Mol Cell Biol. 2015;35(22):3854-65. Epub 2015/09/02. doi: 10.1128/MCB.00706-15. PubMed PMID: 26324326; PubMed Central PMCID: PMCPMC4609739.

30. Dovey OM, Foster CT, Conte N, Edwards SA, Edwards JM, Singh R, et al. Histone deacetylase 1 and 2 are essential for normal T-cell development and genomic stability in mice. Blood. 2013;121(8):1335-44. Epub

2013/01/05. doi: 10.1182/blood-2012-07-441949. PubMed PMID: 23287868; PubMed Central PMCID: PMCPMC3836254.

31. Heideman MR, Wilting RH, Yanover E, Velds A, de Jong J, Kerkhoven RM, et al. Dosage-dependent tumor suppression by histone deacetylases 1 and 2 through regulation of c-Myc collaborating genes and p53 function. Blood. 2013;121(11):2038-50. Epub 2013/01/19. doi: 10.1182/blood-2012-08-450916. PubMed PMID: 23327920; PubMed Central PMCID: PMCPMC3596963.

32. Xiao H, Jiao J, Wang L, O'Brien S, Newick K, Wang LC, et al. HDAC5 controls the functions of Foxp3(+) T-regulatory and CD8(+) T cells. Int J Cancer. 2016;138(10):2477-86. Epub 2015/12/26. doi: 10.1002/ijc.29979. PubMed PMID: 26704363; PubMed Central PMCID: PMCPMC5484398.

33. Tsuji G, Okiyama N, Villarroel VA, Katz SI. Histone deacetylase 6 inhibition impairs effector CD8 T-cell functions during skin inflammation. The Journal of allergy and clinical immunology. 2015;135(5):1228-39. Epub 2014/12/03. doi: 10.1016/j.jaci.2014.10.002. PubMed PMID: 25458911; PubMed Central PMCID: PMCPMC4426217.

34. Nunez-Andrade N, Iborra S, Trullo A, Moreno-Gonzalo O, Calvo E, Catalan E, et al. HDAC6 regulates the dynamics of lytic granules in cytotoxic T lymphocytes. J Cell Sci. 2016;129(7):1305-11. Epub 2016/02/13. doi: 10.1242/jcs.180885. PubMed PMID: 26869226; PubMed Central PMCID: PMCPMC5023047.

35. Tschismarov R, Firner S, Gil-Cruz C, Goschl L, Boucheron N, Steiner G, et al. HDAC1 controls CD8+ T cell homeostasis and antiviral response. PloS one. 2014;9(10):e110576. Epub 2014/10/22. doi: 10.1371/journal.pone.0110576. PubMed PMID: 25333902; PubMed Central PMCID: PMCPMC4204873.

36. Exner V, Aichinger E, Shu H, Wildhaber T, Alfarano P, Caflisch A, et al. The chromodomain of LIKE HETEROCHROMATIN PROTEIN 1 is essential for H3K27me3 binding and function during Arabidopsis development. PloS one. 2009;4(4):e5335. Epub 2009/04/29. doi: 10.1371/journal.pone.0005335. PubMed PMID: 19399177; PubMed Central PMCID: PMCPMC2670505.

37. Hansen KH, Bracken AP, Pasini D, Dietrich N, Gehani SS, Monrad A, et al. A model for transmission of the H3K27me3 epigenetic mark. Nat Cell Biol. 2008;10(11):1291-300. Epub 2008/10/22. doi: 10.1038/ncb1787. PubMed PMID: 18931660.

38. van Dijk K, Marley KE, Jeong BR, Xu J, Hesson J, Cerny RL, et al. Monomethyl histone H3 lysine 4 as an epigenetic mark for silenced euchromatin in Chlamydomonas. The Plant cell. 2005;17(9):2439-53. Epub 2005/08/16. doi: 10.1105/tpc.105.034165. PubMed PMID: 16100335; PubMed Central PMCID: PMCPMC1197426.

39. Nightingale KP, Gendreizig S, White DA, Bradbury C, Hollfelder F, Turner BM. Cross-talk between histone modifications in response to histone deacetylase inhibitors: MLL4 links histone H3 acetylation and histone H3K4 methylation. The Journal of biological chemistry. 2007;282(7):4408-16. Epub 2006/12/15. doi: 10.1074/jbc.M606773200. PubMed PMID: 17166833.

40. Taverna SD, Ilin S, Rogers RS, Tanny JC, Lavender H, Li H, et al. Yng1 PHD finger binding to H3 trimethylated at K4 promotes NuA3 HAT activity at K14 of H3 and transcription at a subset of targeted ORFs. Mol Cell. 2006;24(5):785-96. Epub 2006/12/13. doi: 10.1016/j.molcel.2006.10.026. PubMed PMID: 17157260; PubMed Central PMCID: PMCPMC4690528.

41. Roh TY, Cuddapah S, Cui K, Zhao K. The genomic landscape of histone modifications in human T cells. Proceedings of the National Academy of Sciences of the United States of America. 2006;103(43):15782-7. Epub 2006/10/18. doi: 10.1073/pnas.0607617103. PubMed PMID: 17043231; PubMed Central PMCID: PMCPMC1613230.

42. Akkers RC, van Heeringen SJ, Jacobi UG, Janssen-Megens EM, Francoijs KJ, Stunnenberg HG, et al. A hierarchy of H3K4me3 and H3K27me3 acquisition in spatial gene regulation in Xenopus embryos. Dev Cell. 2009;17(3):425-34. Epub 2009/09/18. doi: 10.1016/j.devcel.2009.08.005. PubMed PMID: 19758566; PubMed Central PMCID: PMCPMC2746918.

43. de la Paz Sanchez M, Gutierrez C. Arabidopsis ORC1 is a PHD-containing H3K4me3 effector that regulates transcription. Proceedings of the National Academy of Sciences of the United States of America. 2009;106(6):2065-70. Epub 2009/01/28. doi: 10.1073/pnas.0811093106. PubMed PMID: 19171893; PubMed Central PMCID: PMCPMC2644164.

44. Strahl BD, Allis CD. The language of covalent histone modifications. Nature. 2000;403(6765):41-5. Epub 2000/01/19. doi: 10.1038/47412. PubMed PMID: 10638745.

45. He S, Tong Q, Bishop DK, Zhang Y. Histone methyltransferase and histone methylation in inflammatory T-cell responses. Immunotherapy. 2013;5(9):989-1004. Epub 2013/09/04. doi: 10.2217/imt.13.101. PubMed PMID: 23998733; PubMed Central PMCID: PMCPMC3879725.

46. Bernstein BE, Mikkelsen TS, Xie X, Kamal M, Huebert DJ, Cuff J, et al. A bivalent chromatin structure marks key developmental genes in embryonic stem cells. Cell. 2006;125(2):315-26. Epub 2006/04/25. doi: 10.1016/j.cell.2006.02.041. PubMed PMID: 16630819.

47. Stock JK, Giadrossi S, Casanova M, Brookes E, Vidal M, Koseki H, et al. Ring1-mediated ubiquitination of H2A restrains poised RNA polymerase II at bivalent genes in mouse ES cells. Nat Cell Biol. 2007;9(12):1428-35. Epub 2007/11/27. doi: 10.1038/ncb1663. PubMed PMID: 18037880.

48. Jorgensen HF, Azuara V, Amoils S, Spivakov M, Terry A, Nesterova T, et al. The impact of chromatin modifiers on the timing of locus replication in mouse embryonic stem cells. Genome Biol. 2007;8(8):R169. Epub 2007/08/21. doi: 10.1186/gb-2007-8-8-r169. PubMed PMID: 17705870; PubMed Central PMCID: PMCPMC2374999.

49. Ueberheide BM, Mollah S. Deciphering the histone code using mass spectrometry. In: Shabanowitz JRYIaJ, editor. International Journal of Mass Spectrometry. Volume 259, Issues 1–3,2007. p. Pages 46-56,.

50. Keating R, Hertz T, Wehenkel M, Harris TL, Edwards BA, McClaren JL, et al. The kinase mTOR modulates the antibody response to provide cross-protective immunity to lethal infection with influenza virus. Nature immunology. 2013;14(12):1266-76. doi: 10.1038/ni.2741. PubMed PMID: 24141387; PubMed Central PMCID: PMC3883080.

51. Tian Z, Tolić N, Zhao R, Moore RJ, Hengel SM, Robinson EW, et al. Enhanced top-down characterization of histone post-translational modifications. Genome Biology. 2012;13(10):R86. doi: 10.1186/gb-2012-13-10-r86.

52. Grant PA, Eberharter A, John S, Cook RG, Turner BM, Workman JL. Expanded lysine acetylation specificity of Gcn5 in native complexes. The Journal of biological chemistry. 1999;274(9):5895-900. Epub 1999/02/20. doi: 10.1074/jbc.274.9.5895. PubMed PMID: 10026213.

53. Zhao Y, Garcia BA. Comprehensive Catalog of Currently Documented Histone Modifications. Cold Spring Harb Perspect Biol. 2015;7(9):a025064. Epub 2015/09/04. doi: 10.1101/cshperspect.a025064. PubMed PMID: 26330523; PubMed Central PMCID: PMCPMC4563710.

54. Tamaru H, Selker EU. A histone H3 methyltransferase controls DNA methylation in Neurospora crassa. Nature. 2001;414(6861):277-83. Epub 2001/11/20. doi: 10.1038/35104508. PubMed PMID: 11713521.

55. Johnson L, Cao X, Jacobsen S. Interplay between two epigenetic marks. DNA methylation and histone H3 lysine 9 methylation. Curr Biol. 2002;12(16):1360-7. Epub 2002/08/27. doi: 10.1016/s0960-9822(02)00976-4. PubMed PMID: 12194816.

56. Barber CM, Turner FB, Wang Y, Hagstrom K, Taverna SD, Mollah S, et al. The enhancement of histone H4 and H2A serine 1 phosphorylation during mitosis and S-phase is evolutionarily conserved. Chromosoma. 2004;112(7):360-71. Epub 2004/05/11. doi: 10.1007/s00412-004-0281-9. PubMed PMID: 15133681.

57. Zhang Y, Griffin K, Mondal N, Parvin JD. Phosphorylation of histone H2A inhibits transcription on chromatin templates. The Journal of biological chemistry. 2004;279(21):21866-72. Epub 2004/03/11. doi: 10.1074/jbc.M400099200. PubMed PMID: 15010469.

58. Clarke AS, Lowell JE, Jacobson SJ, Pillus L. Esa1p is an essential histone acetyltransferase required for cell cycle progression. Mol Cell Biol. 1999;19(4):2515-26. Epub 1999/03/19. doi: 10.1128/mcb.19.4.2515. PubMed PMID: 10082517; PubMed Central PMCID: PMCPMC84044.

59. Kimura A, Horikoshi M. Tip60 acetylates six lysines of a specific class in core histones in vitro. Genes Cells. 1998;3(12):789-800. Epub 1999/03/30. doi: 10.1046/j.1365-2443.1998.00229.x. PubMed PMID: 10096020.

60. Schiltz RL, Mizzen CA, Vassilev A, Cook RG, Allis CD, Nakatani Y. Overlapping but distinct patterns of histone acetylation by the human coactivators p300 and PCAF within nucleosomal substrates. The Journal of biological chemistry. 1999;274(3):1189-92. Epub 1999/01/09. doi: 10.1074/jbc.274.3.1189. PubMed PMID: 9880483.

61. Verreault A, Kaufman PD, Kobayashi R, Stillman B. Nucleosomal DNA regulates the core-histone-binding subunit of the human Hat1 acetyltransferase. Curr Biol. 1998;8(2):96-108. Epub 1998/03/21. doi: 10.1016/s0960-9822(98)70040-5. PubMed PMID: 9427644.

62. Aihara H, Nakagawa T, Mizusaki H, Yoneda M, Kato M, Doiguchi M, et al. Histone H2A T120 Phosphorylation Promotes Oncogenic Transformation via Upregulation of Cyclin D1. Mol Cell. 2016;64(1):176-88. Epub 2016/10/08. doi: 10.1016/j.molcel.2016.09.012. PubMed PMID: 27716482.

63. Zhang M, Liang C, Chen Q, Yan H, Xu J, Zhao H, et al. Histone H2A phosphorylation recruits topoisomerase IIalpha to centromeres to safeguard genomic stability. EMBO J. 2020;39(3):e101863. Epub 2019/11/27. doi: 10.15252/embj.2019101863. PubMed PMID: 31769059; PubMed Central PMCID: PMCPMC6996575.

64. Füllgrabe J, Hajji N, Joseph B. Cracking the death code: apoptosis-related histone modifications. Cell Death & Differentiation. 2010;17(8):1238-43. doi: 10.1038/cdd.2010.58.

65. Beck HC, Nielsen EC, Matthiesen R, Jensen LH, Sehested M, Finn P, et al. Quantitative Proteomic Analysis of Post-translational Modifications of Human Histones. 2006;5(7):1314-25. doi: 10.1074/mcp.M600007-MCP200 %J Molecular & Cellular Proteomics.

66. Zhang L, Eugeni EE, Parthun MR, Freitas MA. Identification of novel histone post-translational modifications by peptide mass fingerprinting. Chromosoma. 2003;112(2):77-86. Epub 2003/08/26. doi: 10.1007/s00412-003-0244-6. PubMed PMID: 12937907.

67. Kim SC, Sprung R, Chen Y, Xu Y, Ball H, Pei J, et al. Substrate and functional diversity of lysine acetylation revealed by a proteomics survey. Mol Cell. 2006;23(4):607-18. Epub 2006/08/19. doi: 10.1016/j.molcel.2006.06.026. PubMed PMID: 16916647.

68. Wisniewski JR, Zougman A, Mann M. Nepsilon-formylation of lysine is a widespread post-translational modification of nuclear proteins occurring at residues involved in regulation of chromatin function. Nucleic acids research. 2008;36(2):570-7. Epub 2007/12/07. doi: 10.1093/nar/gkm1057. PubMed PMID: 18056081; PubMed Central PMCID: PMCPMC2241850.

69. Cheng J, Blum R, Bowman C, Hu D, Shilatifard A, Shen S, et al. A role for H3K4 monomethylation in gene repression and partitioning of chromatin readers. Mol Cell. 2014;53(6):979-92. Epub 2014/03/25. doi: 10.1016/j.molcel.2014.02.032. PubMed PMID: 24656132; PubMed Central PMCID: PMCPMC4031464.

70. Briggs SD, Bryk M, Strahl BD, Cheung WL, Davie JK, Dent SY, et al. Histone H3 lysine 4 methylation is mediated by Set1 and required for cell growth and rDNA silencing in Saccharomyces cerevisiae. Genes & development. 2001;15(24):3286-95. Epub 2001/12/26. doi: 10.1101/gad.940201. PubMed PMID: 11751634; PubMed Central PMCID: PMCPMC312847.

71. Nakamura T, Mori T, Tada S, Krajewski W, Rozovskaia T, Wassell R, et al. ALL-1 is a histone methyltransferase that assembles a supercomplex of proteins involved in transcriptional regulation. Mol Cell. 2002;10(5):1119-28. Epub 2002/11/28. doi: 10.1016/s1097-2765(02)00740-2. PubMed PMID: 12453419.

72. Zhang X, Bernatavichute YV, Cokus S, Pellegrini M, Jacobsen SE. Genome-wide analysis of mono-, di- and trimethylation of histone H3 lysine 4 in Arabidopsis thaliana. Genome Biol. 2009;10(6):R62. Epub 2009/06/11. doi: 10.1186/gb-2009-10-6-r62. PubMed PMID: 19508735; PubMed Central PMCID: PMCPMC2718496.

73. Pace L, Goudot C, Zueva E, Gueguen P, Burgdorf N, Waterfall JJ, et al. The epigenetic control of stemness in CD8⁺ T cell fate commitment. 2018;359(6372):177-86. doi: 10.1126/science.aah6499 %J Science.

74. Ruenjaiman V, Butta P, Leu YW, Pongpanich M, Leelahavanichkul A, Kueanjinda P, et al. Profile of Histone H3 Lysine 4 Trimethylation and the Effect of Lipopolysaccharide/Immune Complex-Activated Macrophages on Endotoxemia. Frontiers in immunology. 2019;10:2956. Epub 2020/01/31. doi: 10.3389/fimmu.2019.02956. PubMed PMID: 31998290; PubMed Central PMCID: PMCPMC6965496.

75. Chen S, Yang J, Wei Y, Wei X. Epigenetic regulation of macrophages: from homeostasis maintenance to host defense. Cell Mol Immunol. 2020;17(1):36-49. Epub 2019/10/31. doi: 10.1038/s41423-019-0315-0. PubMed PMID: 31664225; PubMed Central PMCID: PMCPMC6952359.

76. LaMere SA, Thompson RC, Meng X, Komori HK, Mark A, Salomon DR. H3K27 Methylation Dynamics during CD4 T Cell Activation: Regulation of JAK/STAT and IL12RB2 Expression by JMJD3. Journal of immunology. 2017;199(9):3158-75. Epub 2017/09/28. doi: 10.4049/jimmunol.1700475. PubMed PMID: 28947543; PubMed Central PMCID: PMCPMC5679303.

77. Chang S, Aune TM. Dynamic changes in histone-methylation 'marks' across the locus encoding interferon-gamma during the differentiation of T helper type 2 cells. Nature immunology. 2007;8(7):723-31. Epub 2007/06/05. doi: 10.1038/ni1473. PubMed PMID: 17546034.

78. van der Merwe MM, Smith JE. [The community health nurse in the next decades]. Nurs RSA. 1991;6(6):38-41. Epub 1991/06/01. PubMed PMID: 1876173.

79. Chen X, Wang J, Woltring D, Gerondakis S, Shannon MF. Histone dynamics on the interleukin-2 gene in response to T-cell activation. Mol Cell Biol. 2005;25(8):3209-19. Epub 2005/03/31. doi: 10.1128/MCB.25.8.3209-3219.2005. PubMed PMID: 15798206; PubMed Central PMCID: PMCPMC1069623.

80. Schiza V, Molina-Serrano D, Kyriakou D, Hadjiantoniou A, Kirmizis A. N-alpha-terminal acetylation of histone H4 regulates arginine methylation and ribosomal DNA silencing. PLoS Genet. 2013;9(9):e1003805. Epub 2013/09/27. doi: 10.1371/journal.pgen.1003805. PubMed PMID: 24068969; PubMed Central PMCID: PMCPMC3778019.

81. Ju J, Chen A, Deng Y, Liu M, Wang Y, Wang Y, et al. NatD promotes lung cancer progression by preventing histone H4 serine phosphorylation to activate Slug expression. Nature communications. 2017;8(1):928. Epub 2017/10/17. doi: 10.1038/s41467-017-00988-5. PubMed PMID: 29030587; PubMed Central PMCID: PMCPMC5640650.

82. Olp MD, Zhu N, Smith BC. Metabolically Derived Lysine Acylations and Neighboring Modifications Tune the Binding of the BET Bromodomains to Histone H4. Biochemistry. 2017;56(41):5485-95. Epub 2017/09/26. doi: 10.1021/acs.biochem.7b00595. PubMed PMID: 28945351; PubMed Central PMCID: PMCPMC5970795.

83. Chew YC, Camporeale G, Kothapalli N, Sarath G, Zempleni J. Lysine residues in N-terminal and C-terminal regions of human histone H2A are targets for biotinylation by biotinidase. The Journal of nutritional biochemistry. 2006;17(4):225-33. Epub 2005/08/20. doi: 10.1016/j.jnutbio.2005.05.003. PubMed PMID: 16109483; PubMed Central PMCID: PMCPMC1407762.

84. Kothapalli N, Camporeale G, Kueh A, Chew YC, Oommen AM, Griffin JB, et al. Biological functions of biotinylated histones. The Journal of nutritional biochemistry. 2005;16(7):446-8. Epub 2005/07/05. doi: 10.1016/j.jnutbio.2005.03.025. PubMed PMID: 15992689; PubMed Central PMCID: PMCPMC1226983.

85. Odegard VH, Kim ST, Anderson SM, Shlomchik MJ, Schatz DG. Histone modifications associated with somatic hypermutation. Immunity. 2005;23(1):101-10. Epub 2005/07/26. doi: 10.1016/j.immuni.2005.05.007. PubMed PMID: 16039583.

86. Molden RC, Bhanu NV, LeRoy G, Arnaudo AM, Garcia BA. Multi-faceted quantitative proteomics analysis of histone H2B isoforms and their modifications. Epigenetics Chromatin. 2015;8:15. Epub 2015/04/30. doi: 10.1186/s13072-015-0006-8. PubMed PMID: 25922622; PubMed Central PMCID: PMCPMC4411797.

87. Ruiz PD, Gamble MJ. MacroH2A1 chromatin specification requires its docking domain and acetylation of H2B lysine 20. Nature communications. 2018;9(1):5143. doi: 10.1038/s41467-018-07189-8.

88. Creyghton MP, Cheng AW, Welstead GG, Kooistra T, Carey BW, Steine EJ, et al. Histone H3K27ac separates active from poised enhancers and predicts developmental state. Proceedings of the National Academy of Sciences of the United States of America. 2010;107(50):21931-6. Epub 2010/11/26. doi: 10.1073/pnas.1016071107. PubMed PMID: 21106759; PubMed Central PMCID: PMCPMC3003124.

89. Morris SA, Rao B, Garcia BA, Hake SB, Diaz RL, Shabanowitz J, et al. Identification of histone H3 lysine 36 acetylation as a highly conserved histone modification. The Journal of biological chemistry. 2007;282(10):7632-40. Epub 2006/12/26. doi: 10.1074/jbc.M607909200. PubMed PMID: 17189264; PubMed Central PMCID: PMCPMC2811852.

90. Beisel C, Imhof A, Greene J, Kremmer E, Sauer F. Histone methylation by the Drosophila epigenetic transcriptional regulator Ash1. Nature. 2002;419(6909):857-62. Epub 2002/10/25. doi: 10.1038/nature01126. PubMed PMID: 12397363.

91. Carter JE, Jr. Decreased heart rate variability in congestive heart failure. Am J Cardiol. 1992;69(3):286-7. Epub 1992/01/25. doi: 10.1016/0002-9149(92)91325-x. PubMed PMID: 1731478.

92. Daujat S, Bauer UM, Shah V, Turner B, Berger S, Kouzarides T. Crosstalk between CARM1 methylation and CBP acetylation on histone H3. Curr Biol. 2002;12(24):2090-7. Epub 2002/12/25. doi: 10.1016/s0960-9822(02)01387-8. PubMed PMID: 12498683.

93. Pal S, Vishwanath SN, Erdjument-Bromage H, Tempst P, Sif S. Human SWI/SNF-associated PRMT5 methylates histone H3 arginine 8 and negatively regulates expression of ST7 and NM23 tumor suppressor genes. Mol Cell Biol. 2004;24(21):9630-45. Epub 2004/10/16. doi: 10.1128/MCB.24.21.9630-9645.2004. PubMed PMID: 15485929; PubMed Central PMCID: PMCPMC522266.

94. Teoh PC, Tan LK, Chia BL, Chao TC, Tambyah JA, Feng PH. Non-specific aorto-arteritis in Singapore with special reference to hypertension. Am Heart J. 1978;95(6):683-90. Epub 1978/06/01. doi: 10.1016/0002-8703(78)90496-9. PubMed PMID: 26213.

95. Suka N, Suka Y, Carmen AA, Wu J, Grunstein M. Highly specific antibodies determine histone acetylation site usage in yeast heterochromatin and euchromatin. Mol Cell. 2001;8(2):473-9. Epub 2001/09/08. doi: 10.1016/s1097-2765(01)00301-x. PubMed PMID: 11545749.

96. Rea S, Eisenhaber F, O'Carroll D, Strahl BD, Sun ZW, Schmid M, et al. Regulation of chromatin structure by site-specific histone H3 methyltransferases. Nature. 2000;406(6796):593-9. Epub 2000/08/19. doi: 10.1038/35020506. PubMed PMID: 10949293.

97. Nakayama J, Rice JC, Strahl BD, Allis CD, Grewal SI. Role of histone H3 lysine 9 methylation in epigenetic control of heterochromatin assembly. Science. 2001;292(5514):110-3. Epub 2001/04/03. doi: 10.1126/science.1060118. PubMed PMID: 11283354.

98. Tachibana M, Sugimoto K, Fukushima T, Shinkai Y. Set domain-containing protein, G9a, is a novel lysine-preferring mammalian histone methyltransferase with hyperactivity and specific selectivity to lysines 9 and 27 of

histone H3. The Journal of biological chemistry. 2001;276(27):25309-17. Epub 2001/04/24. doi: 10.1074/jbc.M101914200. PubMed PMID: 11316813.

99. Schultz DC, Ayyanathan K, Negorev D, Maul GG, Rauscher FJ, 3rd. SETDB1: a novel KAP-1-associated histone H3, lysine 9-specific methyltransferase that contributes to HP1-mediated silencing of euchromatic genes by KRAB zinc-finger proteins. Genes & development. 2002;16(8):919-32. Epub 2002/04/18. doi: 10.1101/gad.973302. PubMed PMID: 11959841; PubMed Central PMCID: PMCPMC152359.

100. Cao R, Wang L, Wang H, Xia L, Erdjument-Bromage H, Tempst P, et al. Role of histone H3 lysine 27 methylation in Polycomb-group silencing. Science. 2002;298(5595):1039-43. Epub 2002/09/28. doi: 10.1126/science.1076997. PubMed PMID: 12351676.

101. McKittrick E, Gafken PR, Ahmad K, Henikoff S. Histone H3.3 is enriched in covalent modifications associated with active chromatin. Proceedings of the National Academy of Sciences of the United States of America. 2004;101(6):1525-30. Epub 2004/01/21. doi: 10.1073/pnas.0308092100. PubMed PMID: 14732680; PubMed Central PMCID: PMCPMC341768.

102. Hake SB, Garcia BA, Duncan EM, Kauer M, Dellaire G, Shabanowitz J, et al. Expression patterns and post-translational modifications associated with mammalian histone H3 variants. The Journal of biological chemistry. 2006;281(1):559-68. Epub 2005/11/04. doi: 10.1074/jbc.M509266200. PubMed PMID: 16267050.

103. Wang H, Huang ZQ, Xia L, Feng Q, Erdjument-Bromage H, Strahl BD, et al. Methylation of histone H4 at arginine 3 facilitating transcriptional activation by nuclear hormone receptor. Science. 2001;293(5531):853-7. Epub 2001/06/02. doi: 10.1126/science.1060781. PubMed PMID: 11387442.

104. Strahl BD, Briggs SD, Brame CJ, Caldwell JA, Koh SS, Ma H, et al. Methylation of histone H4 at arginine 3 occurs in vivo and is mediated by the nuclear receptor coactivator PRMT1. Curr Biol. 2001;11(12):996-1000. Epub 2001/07/13. doi: 10.1016/s0960-9822(01)00294-9. PubMed PMID: 11448779.

105. Nishioka K, Rice JC, Sarma K, Erdjument-Bromage H, Werner J, Wang Y, et al. PR-Set7 is a nucleosome-specific methyltransferase that modifies lysine 20 of histone H4 and is associated with silent chromatin. Mol Cell. 2002;9(6):1201-13. Epub 2002/06/28. doi: 10.1016/s1097-2765(02)00548-8. PubMed PMID: 12086618.

106. Schotta G, Lachner M, Sarma K, Ebert A, Sengupta R, Reuter G, et al. A silencing pathway to induce H3-K9 and H4-K20 trimethylation at constitutive heterochromatin. Genes & development. 2004;18(11):1251-62. Epub 2004/05/18. doi: 10.1101/gad.300704. PubMed PMID: 15145825; PubMed Central PMCID: PMCPMC420351.

107. Fang J, Feng Q, Ketel CS, Wang H, Cao R, Xia L, et al. Purification and functional characterization of SET8, a nucleosomal histone H4-lysine 20-specific methyltransferase. Curr Biol. 2002;12(13):1086-99. Epub 2002/07/18. doi: 10.1016/s0960-9822(02)00924-7. PubMed PMID: 12121615.

108. Volgin Iu B, Rethy L, Raskai M. [Comparative immunochemical study of the antigenic makeup of native tetanus toxin from sporulating and nonsporulating C1. tetani strains]. Zh Mikrobiol Epidemiol Immunobiol. 1976;(6):47-51. Epub 1976/06/01. PubMed PMID: 821277.

109. Kuo MH, Brownell JE, Sobel RE, Ranalli TA, Cook RG, Edmondson DG, et al. Transcription-linked acetylation by Gcn5p of histones H3 and H4 at specific lysines. Nature. 1996;383(6597):269-72. Epub 1996/09/19. doi: 10.1038/383269a0. PubMed PMID: 8805705.

110. Winkler GS, Kristjuhan A, Erdjument-Bromage H, Tempst P, Svejstrup JQ. Elongator is a histone H3 and H4 acetyltransferase important for normal histone acetylation levels in vivo. Proceedings of the National Academy of Sciences of the United States of America. 2002;99(6):3517-22. Epub 2002/03/21. doi: 10.1073/pnas.022042899. PubMed PMID: 11904415; PubMed Central PMCID: PMCPMC122555.

111. Hilfiker A, Hilfiker-Kleiner D, Pannuti A, Lucchesi JC. mof, a putative acetyl transferase gene related to the Tip60 and MOZ human genes and to the SAS genes of yeast, is required for dosage compensation in Drosophila.

EMBO J. 1997;16(8):2054-60. Epub 1997/04/15. doi: 10.1093/emboj/16.8.2054. PubMed PMID: 9155031; PubMed Central PMCID: PMCPMC1169808.

112. Alaskhar Alhamwe B, Khalaila R, Wolf J, von Bulow V, Harb H, Alhamdan F, et al. Histone modifications and their role in epigenetics of atopy and allergic diseases. Allergy Asthma Clin Immunol. 2018;14:39. Epub 2018/05/26. doi: 10.1186/s13223-018-0259-4. PubMed PMID: 29796022; PubMed Central PMCID: PMCPMC5966915.

113. Schafer A, Baric RS. Epigenetic Landscape during Coronavirus Infection. Pathogens. 2017;6(1). Epub 2017/02/18. doi: 10.3390/pathogens6010008. PubMed PMID: 28212305; PubMed Central PMCID: PMCPMC5371896.

114. Zhang YH, Meng JL, Gao Y, Zhang JY, Niu SL, Yu XZ, et al. Changes in methylation of genomic DNA from chicken immune organs in response to H5N1 influenza virus infection. Genet Mol Res. 2016;15(3). Epub 2016/10/06. doi: 10.4238/gmr.15037382. PubMed PMID: 27706718.

115. Mukherjee S, Vipat VC, Chakrabarti AK. Infection with influenza A viruses causes changes in promoter DNA methylation of inflammatory genes. Influenza Other Respir Viruses. 2013;7(6):979-86. Epub 2013/06/14. doi: 10.1111/irv.12127. PubMed PMID: 23758996; PubMed Central PMCID: PMCPMC4634256.

116. Tang B, Zhao R, Sun Y, Zhu Y, Zhong J, Zhao G, et al. Interleukin-6 expression was regulated by epigenetic mechanisms in response to influenza virus infection or dsRNA treatment. Mol Immunol. 2011;48(8):1001-8. Epub 2011/03/01. doi: 10.1016/j.molimm.2011.01.003. PubMed PMID: 21353307.

117. Menachery VD, Eisfeld AJ, Schafer A, Josset L, Sims AC, Proll S, et al. Pathogenic influenza viruses and coronaviruses utilize similar and contrasting approaches to control interferon-stimulated gene responses. mBio. 2014;5(3):e01174-14. Epub 2014/05/23. doi: 10.1128/mBio.01174-14. PubMed PMID: 24846384; PubMed Central PMCID: PMCPMC4030454.

118. Marcos-Villar L, Diaz-Colunga J, Sandoval J, Zamarreno N, Landeras-Bueno S, Esteller M, et al. Epigenetic control of influenza virus: role of H3K79 methylation in interferon-induced antiviral response. Scientific reports. 2018;8(1):1230. Epub 2018/01/21. doi: 10.1038/s41598-018-19370-6. PubMed PMID: 29352168; PubMed Central PMCID: PMCPMC5775356.

119. Marcos-Villar L, Pazo A, Nieto A. Influenza Virus and Chromatin: Role of the CHD1 Chromatin Remodeler in the Virus Life Cycle. Journal of virology. 2016;90(7):3694-707. Epub 2016/01/23. doi: 10.1128/JVI.00053-16. PubMed PMID: 26792750; PubMed Central PMCID: PMCPMC4794673.

120. Huarte M, Sanz-Ezquerro JJ, Roncal F, Ortin J, Nieto A. PA subunit from influenza virus polymerase complex interacts with a cellular protein with homology to a family of transcriptional activators. Journal of virology. 2001;75(18):8597-604. Epub 2001/08/17. doi: 10.1128/jvi.75.18.8597-8604.2001. PubMed PMID: 11507205; PubMed Central PMCID: PMCPMC115105.

121. Alfonso R, Lutz T, Rodriguez A, Chavez JP, Rodriguez P, Gutierrez S, et al. CHD6 chromatin remodeler is a negative modulator of influenza virus replication that relocates to inactive chromatin upon infection. Cell Microbiol. 2011;13(12):1894-906. Epub 2011/09/09. doi: 10.1111/j.1462-5822.2011.01679.x. PubMed PMID: 21899694.

122. Chandele A, Joshi NS, Zhu J, Paul WE, Leonard WJ, Kaech SM. Formation of IL-7Ralphahigh and IL-7Ralphalow CD8 T cells during infection is regulated by the opposing functions of GABPalpha and Gfi-1. Journal of immunology. 2008;180(8):5309-19. Epub 2008/04/09. doi: 10.4049/jimmunol.180.8.5309. PubMed PMID: 18390712; PubMed Central PMCID: PMCPMC2792750.

123. Navarro MN, Goebel J, Feijoo-Carnero C, Morrice N, Cantrell DA. Phosphoproteomic analysis reveals an intrinsic pathway for the regulation of histone deacetylase 7 that controls the function of cytotoxic T lymphocytes. Nature immunology. 2011;12(4):352-61. Epub 2011/03/15. doi: 10.1038/ni.2008. PubMed PMID: 21399638; PubMed Central PMCID: PMCPMC3110993.

124. Eberharter A, Becker PB. Histone acetylation: a switch between repressive and permissive chromatin. Second in review series on chromatin dynamics. 2002;3(3):224-9. Epub 2002/03/08. doi: 10.1093/embo-reports/kvf053. PubMed PMID: 11882541; PubMed Central PMCID: PMCPMC1084017.

125. Bannister AJ, Kouzarides T. Regulation of chromatin by histone modifications. Cell Res. 2011;21(3):381-95. Epub 2011/02/16. doi: 10.1038/cr.2011.22. PubMed PMID: 21321607; PubMed Central PMCID: PMCPMC3193420.

126. Gray SM, Kaech SM, Staron MM. The interface between transcriptional and epigenetic control of effector and memory CD8(+) T-cell differentiation. Immunol Rev. 2014;261(1):157-68. Epub 2014/08/16. doi: 10.1111/imr.12205. PubMed PMID: 25123283; PubMed Central PMCID: PMCPMC4267690.

127. Turner BM. Cellular memory and the histone code. Cell. 2002;111(3):285-91. Epub 2002/11/07. doi: 10.1016/s0092-8674(02)01080-2. PubMed PMID: 12419240.

128. Su X, Ren C, Freitas MA. Mass spectrometry-based strategies for characterization of histones and their post-translational modifications. Expert Rev Proteomics. 2007;4(2):211-25. Epub 2007/04/12. doi: 10.1586/14789450.4.2.211. PubMed PMID: 17425457; PubMed Central PMCID: PMCPMC2572816.

129. Sidoli S, Vandamme J, Salcini AE, Jensen ON. Dynamic changes of histone H3 marks during Caenorhabditis elegans lifecycle revealed by middle-down proteomics. Proteomics. 2016;16(3):459-64. Epub 2015/10/29. doi: 10.1002/pmic.201500285. PubMed PMID: 26508544.

130. Schwammle V, Sidoli S, Ruminowicz C, Wu X, Lee CF, Helin K, et al. Systems Level Analysis of Histone H3 Post-translational Modifications (PTMs) Reveals Features of PTM Crosstalk in Chromatin Regulation. Molecular & cellular proteomics : MCP. 2016;15(8):2715-29. Epub 2016/06/16. doi: 10.1074/mcp.M115.054460. PubMed PMID: 27302890; PubMed Central PMCID: PMCPMC4974346.

131. Sidoli S, Lopes M, Lund PJ, Goldman N, Fasolino M, Coradin M, et al. A mass spectrometry-based assay using metabolic labeling to rapidly monitor chromatin accessibility of modified histone proteins. Scientific reports. 2019;9(1):13613. Epub 2019/09/22. doi: 10.1038/s41598-019-49894-4. PubMed PMID: 31541121; PubMed Central PMCID: PMCPMC6754405.